

Modifications on the amino-3,5-dicyanopyridine core to obtain multifaceted adenosine receptor ligands with antineuropathic activity

Marco Betti, Daniela Catarzi, Flavia Varano, Matteo Falsini, Katia Varani, Fabrizio Vincenzi, Silvia Pasquini, Lorenzo Di Cesare Mannelli, Carla Ghelardini, Elena Lucarini, Diego Dal Ben, Andrea Spinaci, Gianluca Bartolucci, Marta Menicatti, and Vittoria Colotta

J. Med. Chem., **Just Accepted Manuscript** • DOI: 10.1021/acs.jmedchem.9b00106 • Publication Date (Web): 15 Jul 2019

Downloaded from pubs.acs.org on July 22, 2019

Just Accepted

“Just Accepted” manuscripts have been peer-reviewed and accepted for publication. They are posted online prior to technical editing, formatting for publication and author proofing. The American Chemical Society provides “Just Accepted” as a service to the research community to expedite the dissemination of scientific material as soon as possible after acceptance. “Just Accepted” manuscripts appear in full in PDF format accompanied by an HTML abstract. “Just Accepted” manuscripts have been fully peer reviewed, but should not be considered the official version of record. They are citable by the Digital Object Identifier (DOI®). “Just Accepted” is an optional service offered to authors. Therefore, the “Just Accepted” Web site may not include all articles that will be published in the journal. After a manuscript is technically edited and formatted, it will be removed from the “Just Accepted” Web site and published as an ASAP article. Note that technical editing may introduce minor changes to the manuscript text and/or graphics which could affect content, and all legal disclaimers and ethical guidelines that apply to the journal pertain. ACS cannot be held responsible for errors or consequences arising from the use of information contained in these “Just Accepted” manuscripts.

1
2
3 **Modifications on the amino-3,5-dicyanopyridine core to obtain**
4 **multifaceted adenosine receptor ligands with antineuropathic**
5 **activity**
6
7
8
9

10
11 Marco Betti,^a Daniela Catarzi,^{a*} Flavia Varano,^a Matteo Falsini,^a Katia Varani,^b Fabrizio Vincenzi,^b
12 Silvia Pasquini,^b Lorenzo di Cesare Mannelli,^c Carla Ghelardini,^c Elena Lucarini,^c
13 Diego Dal Ben,^d Andrea Spinaci,^d Gianluca Bartolucci,^a Marta Menicatti,^a Vittoria Colotta^a
14
15
16
17

18 ^a*Dipartimento di Neuroscienze, Psicologia, Area del Farmaco e Salute del Bambino, Sezione di Farmaceutica e*
19 *Nutraceutica, Università degli Studi di Firenze, Via Ugo Schiff, 6, 50019 Sesto Fiorentino, Italy.*

20 ^b*Dipartimento di Scienze Mediche, Sezione di Farmacologia, Università degli Studi di Ferrara, Via Fossato di Mortara*
21 *17-19, 44121 Ferrara, Italy*

22 ^c*Dipartimento di Neuroscienze, Psicologia, Area del Farmaco e Salute del Bambino, Sezione di Farmacologia e*
23 *Tossicologia, Università degli Studi di Firenze, Viale Pieraccini, 6, 50139 Firenze, Italy.*

24 ^d*Scuola di Scienze del Farmaco e dei Prodotti della Salute, Università degli Studi di Camerino, Via S. Agostino 1,*
25 *62032 Camerino (MC), Italy.*
26
27
28
29
30
31
32
33
34
35
36

37 **Key words:** G protein-coupled receptors, adenosine receptor ligands, aminopyridine-3,5-
38 dicarbonitriles, ligand-adenosine receptor modeling studies, neuropathic pain.
39
40
41
42

43 Corresponding author e-mail: daniela.catarzi@unifi.it.
44
45
46
47
48
49
50
51
52
53
54
55
56
57
58
59
60

Abstract.

A new series of amino-3,5-dicyanopyridines (**1-31**) was synthesized and biologically evaluated in order to further investigate the potential of this scaffold to obtain adenosine receptor (AR) ligands. In general, the modifications performed have led to compounds having from high to good human (h) A₁AR affinity and an inverse agonist profile. While most of the compounds are hA₁AR selective, some derivatives behave as mixed hA₁AR inverse agonists/A_{2A} and A_{2B} AR antagonists. These latter (compound **9-12**) showed to reduce oxaliplatin-induced neuropathic pain by a mechanism involving the alpha7 subtype of nAChRs, similarly to the non-selective AR antagonist caffeine, taken as reference compound. Along with the pharmacological evaluation, chemical stability of the methyl 3-(((6-amino-3,5-dicyano-4-(furan-2-yl)pyridin-2-yl)sulfanyl)methyl)benzoate **10** was assessed in plasma matrices (rat and human), and molecular modeling studies were carried out to better rationalize the available SARs.

INTRODUCTION

Adenosine is an endogenous autocooid as regulating the function of every tissue and organ in the body.¹ Under physiological conditions, adenosine is present in the extracellular space at low concentrations which dramatically increase in response to stress. Thus, it interacts with specific G protein-coupled adenosine receptors (ARs), four subtypes currently recognized and termed A₁, A_{2A}, A_{2B}, and A₃ ARs. Under physiological conditions, concentration of extracellular adenosine (0.3-1000 nM) is high enough to activate both the A₁ and A_{2A} ARs. In contrast, the low affinity A_{2B} and A₃ subtypes require higher concentrations of extracellular nucleoside. All ARs affect cAMP levels, A₁ and A₃ receptors being coupled to inhibitory G_i, and A_{2A} and A_{2B} receptors to stimulatory G_s proteins, respectively. Furthermore, A₃ and A_{2B} receptors are also coupled to G_q proteins, leading to the activation of phospholipase C (PLC) and an increase in calcium levels.^{1,2} Coupling to other intracellular signaling pathways has also been described.² The cloning of the four AR subtypes has allowed for significant progress to be made in the understanding of several facets of AR activity at a molecular level. It is well documented that the activation of ARs can produce a large variety of effects in different tissues and organs. The widely diffused adenosine signaling has left long hypothesize that the regulation of ARs' activity had a high therapeutic potential. However, this ubiquity makes the development of selective AR agonists and antagonists difficult to realize without the occurrence of side effects.³

The use of AR agonists and antagonists has been shown to protect against neurodegenerative pathologies such as Alzheimer's and Parkinson's diseases, and also neurological insult caused by spinal cord injury and stroke.^{4,5} Experimental evidence supports the use of AR antagonists as well as agonists in the control of inflammatory response, sensory and motor deficits, hyperalgesia, antinociception and excitotoxicity related to specific neurodegenerative disorders.⁶⁻¹¹ Results obtained up to now have allowed the seemingly paradoxical use of agonists and antagonists of the same AR subtype to treat similar pathologies to emerge. These contrasting approaches suggest that the state of disease progression, dosage and time of drug application, drug delivery method and many

1
2
3 other factors could be critical for the design of the most effective therapy. In recent years, there have
4
5 been significant developments that enhance an understanding of the role of adenosine in nociception.
6
7 It has emerged that all the four AR subtypes are involved in pain regulation but with different roles.¹¹
8
9 Some experimental evidence suggests the role of both A₁ and A_{2A} ARs as key targets for the
10
11 regulation of pain, leaving however the debate about the pharmacological use of agonists and/or
12
13 antagonists open.¹²⁻¹⁷
14
15

16
17 Among the four ARs, the A₁ subtype has been traditionally described as a neuroprotective receptor¹⁸
18
19 while the excitatory effect of the A_{2A}AR in neurodegeneration has been preferentially reported.^{4,5}
20
21 However, some evidence suggested that prolonged A₁AR activation may led to neurodegeneration,
22
23 leading to hypothesize an apparent A₁/A_{2A} ARs cross-talk.¹⁹ In this situation, the A₁ signaling
24
25 enhances the A_{2A}-mediated neurodegeneration. Also the effect on neurotransmitter release is the
26
27 opposite: activation of the A₁ subtype is associated with inhibition while the A_{2A}AR promotes an
28
29 increased release.²⁰
30
31

32
33 Since the 1990s, much effort has been devoted to evaluating the pharmacological actions of caffeine,
34
35 the most consumed psychoactive legal drug in the world.¹² Its neuroprotective effects have been
36
37 generally ascribed to the blockade of both the A₁ and A_{2A} ARs though caffeine works as a non-
38
39 selective antagonists of all the four AR subtypes in human. In rodents, the lack of affinity only for
40
41 the A₃AR was demonstrated.²¹ Also the blockade of the A_{2B} AR was reported to produce
42
43 antinociception in several model of pain.^{11,13} Caffeine's role in controlling pain has been scarcely
44
45 considered in the past yet it is being studied increasingly.^{12,22-25} However, at present the
46
47 antinociceptive activity of AR antagonists such as caffeine is in contrast with the more documented
48
49 pain-protective action exerted by AR agonists, in particular compounds targeting the A₁
50
51 subtype.^{10,11,15,16,18,19}
52
53

54
55 In our laboratory, much research has been addressed to the study of AR ligands belonging to different
56
57 chemical classes²⁶⁻³⁷ including the recently reported amino-3,5-dicyanopyridine series.³⁷ These
58
59 derivatives were designed as hA_{2B}AR agonists although special attention was devoted to deepening
60

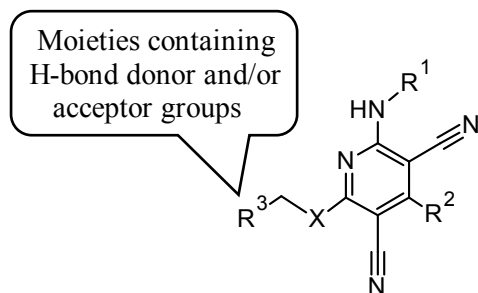
1
2
3 the structure-activity relationships (SARs) of this chemical class. Despite scarce data being reported
4
5 in the open literature,³⁸⁻⁴⁰ the amino-3,5-dicyanopyridine scaffold has showed to be very versatile for
6
7 designing AR ligands. In fact, the compounds, whose pharmacological studies are available to the
8
9 scientific community, may show, in general, not only a wide range of affinities but also different
10
11 degrees of efficacy at the different ARs. In our recent publication³⁷ we reported some potent hA_{2B} AR
12
13 receptor partial agonists, belonging to the amino-3,5-dicyanopyridine series, some of which also
14
15 characterized by good selectivity versus the other AR subtypes. The SAR study highlighted that the
16
17 4-(*para*-cyclopropylmethoxy)phenyl group (Chart 1), with respect to other examined R²
18
19 substituents, emerged as the best one to increase hA_{2B} AR activity and selectivity of the amino-3,5-
20
21 dicyanopyridine compounds. Moreover, moieties bearing H-bond donor and/or acceptor groups at
22
23 R³, able to give polar interactions at this level, proved to be important for A_{2B} receptor ligand
24
25 potency.^{41,42} Thus, we decided to further explore this scaffold to evaluate how modifications at the
26
27 dicyanopyridine core could modulate affinity and selectivity, but also the pharmacological profile of
28
29 these derivatives at the AR subtypes (Chart 1). Maintaining the characteristics of polarity of the R³
30
31 substituents, that could be important not only for the AR interaction but also activation, different
32
33 substituents have been evaluated with attention at the R² position where less explored heteroaryl
34
35 moieties were introduced. Further modifications concerned the linker X and the R¹ substituent
36
37 appended on the amine function.
38
39
40
41
42
43

44 The new derivatives **1-31** were tested to evaluate their affinities at hA₁, hA_{2A} and hA₃ ARs and their
45
46 efficacy at the hA_{2B}AR. Selected compounds (**1, 7-11, 13, 14, 17, 18, 20, 23, 24, 26, 28** and **30**) were
47
48 also analyzed to assess their pharmacological profile at the different ARs. Anticipating our results, it
49
50 emerges that some amino-3,5-dicyanopyridines reported herein (compounds **9-12**) behave as mixed
51
52 hA₁ AR inverse agonists/A_{2A} and A_{2B} AR antagonists. It has to be noted that inverse agonism is
53
54 slowly establishing its physiological role and also taking a place in drug therapy. In fact, it represents
55
56 an important expression of drug-receptor interaction different than that of antagonism. An inverse
57
58 agonist, in addition to blocking the action of the agonist as a neutral antagonist, is able to inhibit the
59
60

constitutive activity of the receptor thus showing negative intrinsic activity. However, if the receptor does not display constitutive activity, the inverse agonist behaves as an antagonist. Moreover, new SARs for inverse agonists versus those for antagonists must be sought for and established. Many compounds, endowed with important therapeutic actions and assumed to be G protein-coupled receptor antagonists, have been successively proved to be inverse agonists. Hence, in light of the previously advanced consideration, we glimpsed the possibility that our compounds could act like caffeine and represent promising candidates for the treatment of neuropathic pain. Thus, derivatives **9-12** were pharmacologically evaluated in an *in vivo* mouse model of oxaliplatin-induced neuropathy. Moreover, the stability of the ethyl ester derivatives **10** was assessed in plasma matrices (rat and human). A molecular modeling study of the new amino-3,5-dicyanopyridine derivatives was performed in order to rationalize the obtained pharmacological results.

Chart 1.

Previously and currently reported amino-3,5-dicyanopyridines as AR ligands.



Previously reported

$R^1 = \text{H}$, $X = \text{S}$
 $R^2 = 4\text{-R}''\text{-C}_6\text{H}_4$
 $R = \text{-O-(cyclo)alkyl}$,
 -O-alkenyl ,
 -NHCOCH_3

Currently reported 1-31

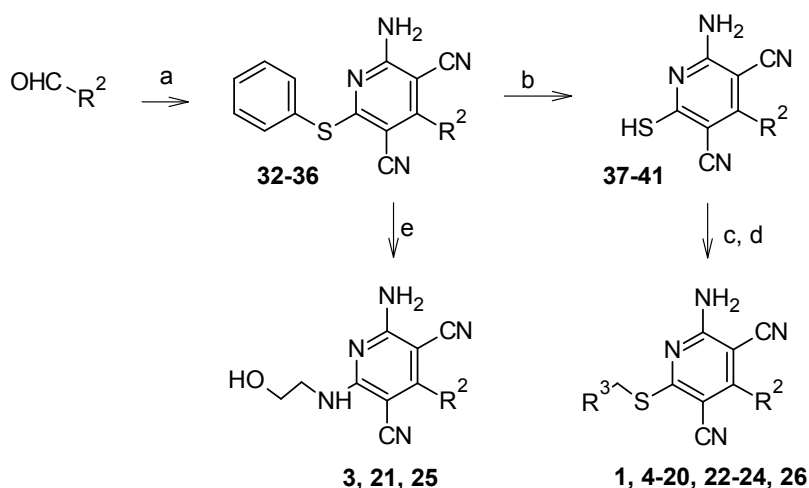
$R^1 = \text{H}$, cycloalkyl, aryl,
 benzyl, acetyl
 $X = \text{S}$, NH , O
 $R^2 = \text{heteroaryl}$

RESULTS AND DISCUSSION.

Chemistry.

The synthetic routes which provided the amino-3,5-dicyanpyridine derivatives **1-31**⁴³⁻⁴⁵ are depicted in Schemes 1-4. Compounds **1, 3-26** (Scheme 1) were synthesized starting from a one-pot cyclization of the suitable commercially available heteroarylaldehyde with malononitrile and thiophenol in the presence of tetra-n-butylammonium fluoride hydrate (TBAF•H₂O) to yield the phenylthio-intermediates **32-36**.⁴⁶⁻⁴⁸ To obtain the free thiols (compounds **37-41**),⁴⁹⁻⁵¹ the corresponding 6-phenylthio-derivatives **32-36** were treated with sodium sulfide in anhydrous DMF at 80 °C followed by treatment with 1N HCl. The final compounds **1, 4-20, 22-24, 26** were obtained in high yield by reacting **37-41** with the suitable halides, (all commercially available), in the presence of sodium hydrogen carbonate or potassium hydroxide (compound **5**). Bromomethyl derivatives were used to prepare compounds **1, 2, 9, 10, 18-20, 22-24, 26**, while to yield derivatives **15-17** chloromethyl intermediates were employed, sometimes as hydrochloride. To test the replacement of the thiomethyl bridge with an aminomethyl linker, compounds **3, 21**,⁴⁵ **25** were synthesized starting from intermediates **32**,⁴⁶ **34**,⁴⁶ **36**⁴⁸ respectively, taking advantage of the good property of phenylthio group as leaving group in a nucleophilic substitution. The reaction was performed at 100 °C in DMF using 2-aminoethanol as nucleophile.

Scheme 1.

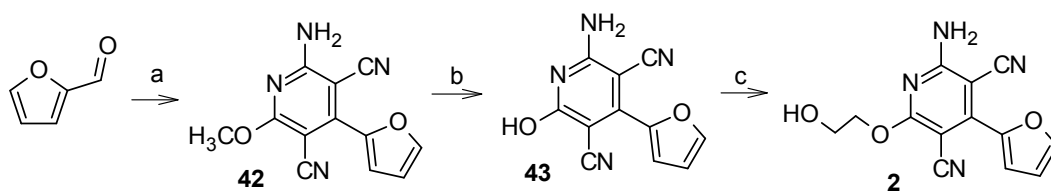


R^2	compd	R^2	compd
	1,3-17, 32, 37		23, 35, 40
	18, 19, 33, 38		24-26, 36, 41
	20-22, 34, 39		

Reagents and conditions. a) Malononitrile, thiophenol, TBAF, H_2O , $80\text{ }^\circ\text{C}$; b) Na_2S , anhydrous DMF, $80\text{ }^\circ\text{C}$; 1N HCl, rt; c) $\text{R}^3\text{CH}_2\text{Br}$, NaHCO_3 , anhydrous DMF, rt; d) $\text{NH}_2\text{COCH}_2\text{Cl}$, 10% KOH, DMF, rt (compound **5**); e) $\text{NH}_2\text{CH}_2\text{CH}_2\text{OH}$, DMF, $100\text{ }^\circ\text{C}$; (for R^3 substituent details see Table 1).

Pursuing modifications at the methylthio linker, compound **2**, bearing a methoxyethanol chain was synthesized (Scheme 2). One-pot cyclization of commercial 2-furaldehyde with malononitrile in the presence of NaOCH_3 yielded intermediate **42**⁵² which was converted into the corresponding hydroxy-analogue **43**⁵³ by treatment with a mixture of concentrated HCl and glacial acetic acid at $100\text{ }^\circ\text{C}$. Hence, **43** was used as starting material for the coupling reaction with 2-bromoethanol, performed in a microwave reactor, to give the final compound **2**.

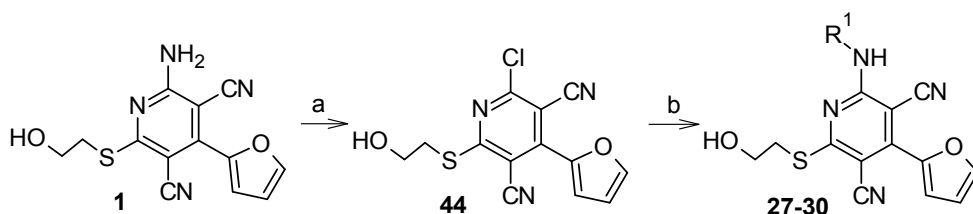
Scheme 2.



Reagents and conditions. a) malononitrile, NaOCH₃, TBAF, MeOH, reflux; b) 12N HCl, glacial AcOH, 100 °C; c) BrCH₂CH₂OH, NaHCO₃, anhydrous DMF, 80 °C, microwave irradiation.

Replacement of the primary amine function of **1** with suitably substituted amino groups was performed to obtain compounds **27-30** (Scheme 3). Diazotization of the amine derivative **1** using isoamylnitrite as nitrosonium donor compound, followed by Sandmeyer reaction with copper (II) chloride afforded compound **44** in good yields. Thus, the chlorine atom of **44** was easily replaced with commercially available substituted amines yielding the final compounds **27-30**.

Scheme 3.



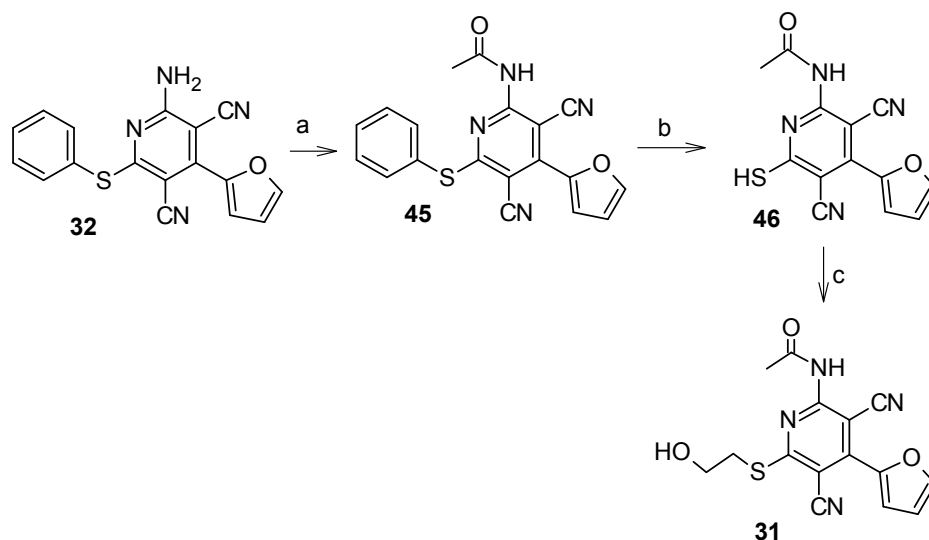
R¹				
compd	27	28	29	30

Reagents and conditions. a) isoamylnitrite, CuCl₂, CH₃CN, rt; b) R¹-NH₂, anhydrous DMF, rt.

Finally, derivative **31**, bearing an acetyl moiety on the amino group, was synthesized as reported in Scheme 4. Reaction of the phenylthio derivative **32** with acetic anhydride in the presence of pyridine produced **45** which was converted into the corresponding thiol analogue **46**⁵⁴ by reacting with sodium

sulfide in anhydrous DMF at 50 °C, followed by treatment with 1N HCl. Then, **46** was used as starting material for the coupling reaction with 2-bromoethanol to afford the target compound **31**.

Scheme 4.



Reagents and conditions. a) acetic anhydride, pyridine, reflux; b) Na_2S , anhydrous DMF, 50 °C; 1N HCl, rt; c) $\text{BrCH}_2\text{CH}_2\text{OH}$, NaHCO_3 , anhydrous DMF, rt.

Pharmacological Assays

The amino-3,5-dicyanopyridines **1-31** were tested for their affinity at hA_1 , hA_{2A} and hA_3 ARs, stably transfected in Chinese Hamster Ovary (CHO) cells, and were also studied as hA_{2B} agonists by evaluating their stimulatory effect on cAMP production in CHO cells, stably expressing the hA_{2B} AR. Some selected compounds (**1**, **3**, **9-11**, **15**, **18** and **21**) were evaluated also in cAMP production in hA_{2B} CHO cells to investigate their antagonistic effect on cAMP production stimulated by 5'-(N-ethyl-carboxamido)adenosine (NECA) 100 nM. Compounds **1**, **3**, **7-24**, **26**, **28**, and **30**, the most interesting in terms of hA_1 AR affinity, were evaluated for their A_1 pharmacological profile in the cAMP assay where each compound was tested to assess its capability to modulate Forskolin-stimulated cAMP levels in the absence or presence of the A_1 AR agonist 2-chloro- N^6 -cyclopentyladenosine (CCPA) (1

nM). Moreover, derivatives **9-11** and **16**, showing good hA_{2A}AR affinity, were evaluated for their ability to inhibit the A_{2A}AR agonist CGS 21680-stimulated cAMP levels in hA_{2A}CHO cells.

All pharmacological data are reported in Tables 1-4 and Figure 1. The selected derivatives **9-12** were also profiled for their effect in an oxaliplatin-induced neuropathic pain model. The results of these experiments are reported in Figures 6-9.

Structure-activity relationships

The pharmacological data reported in Table 1 show that most of the compounds have, in general, null hA_{2B}AR ability in stimulating cAMP production with the only exceptions being derivatives **18**, **20** and **22** that however behave as weak partial agonists. Selected compounds were also evaluated in cAMP assays as hA_{2B}AR antagonists (Table 2). In particular, derivatives **9** and **11** are able to inhibit NECA-stimulated cAMP levels with IC₅₀ values of 152 and 13nM, respectively. In contrast, compounds **1**, **3**, **10**, **15**, **18** and **21** show a percentage of inhibition at the 1 μM concentration in the range 4-40%. Some derivatives (**5**, **6**, **11-13**, **15-17**, **20**, **27** and **31**) interact with the hA₃AR showing in general K_i values in the high nanomolar range (Table 1).

Best results have been obtained in the A₁ and A_{2A} AR binding experiments. In particular, all the compounds reported herein, with the only exception being derivatives **3** and **25**, have from high to good hA₁AR affinity. In particular, some compounds showed K_i values in the low nanomolar range and in general below 10 nM. Compounds **1**, **7-14**, **16-20**, **22-26**, **28** and **30**, the most interesting in terms of affinity at the hA₁AR, were evaluated for their pharmacological behavior toward this receptor subtype. The data reported in Table 3 indicated that potencies of the tested compounds correlate well with the K_i values obtained in the hA₁ binding experiments. All compounds (**1**, **7-14**, **16-20** and **22-26**) were able to increase Forskolin-stimulated cAMP levels in the absence of an agonist, suggesting their inverse agonist profile, with the exception of derivatives **28** (IC₅₀ = 118 ± 9 nM, E_{max} = 100%) and **30** (IC₅₀ = 76 ± 6 nM, E_{max} = 100%) that counteract hA₁AR agonist CCPA inhibition of Forskolin-stimulated cAMP levels behaving as antagonists. The competition curves of

1
2
3 specific [^3H]-DPCPX binding to hA₁ AR of compounds **9-12**, selected for in vivo studies, and their
4
5 effect on forskolin-stimulated c-AMP levels in hA₁AR CHO cells were reported in Figure 1. While
6
7 some compounds are selective hA₁AR inverse agonists, many derivatives bind also the hA_{2A} receptor,
8
9 leading to a series of mixed (but not generally balanced) hA₁/A_{2A} AR ligands. In fact, some
10
11 compounds bind the hA₁AR better than the hA_{2A} one, thus maintaining a certain selectivity. However,
12
13 selected compounds (**9-11**, **16**) were also tested in the cAMP functional assay, revealing their
14
15 antagonistic activity at the hA_{2A}AR (Table 4). The novel compounds were not able to modulate cAMP
16
17 levels in wild type CHO cells suggesting the direct involvement of ARs.
18
19

20
21 Taking into consideration the results that emerged from our previous study on the amino-3,5-
22
23 dicyanopyridine derivatives³⁷ together with those reported in the literature on this class of
24
25 compounds,³⁸⁻⁴⁰ modifications were performed at R² and R³ positions (compounds **1-26**). In
26
27 particular, while poorly investigated heteroaryl substituents were introduced at R², position R³
28
29 generally contains groups or atoms able to engage hydrogen bonds with the receptor site, this latter
30
31 being a condition that seems mandatory for the AR-ligand interaction. First of all, the 2-furanyl
32
33 substituent was evaluated (compounds **1-17**). In fact, by maintaining the 2-furanyl moiety at R²,
34
35 different groups were inserted at R³ position. In general, the presence of the 2-furanyl moiety at R²,
36
37 replacing the classical phenyl or phenyl substituted groups usually present at this position, seems to
38
39 highly influence the interaction or the modality of interaction with the hA_{2B}AR. In fact, 4-(2-furanyl)-
40
41 substituted compounds lose the capability to activate this AR subtype, while some, selectively tested
42
43 derivatives (**9** and **11**) behaved as hA_{2B} antagonists.
44
45
46
47
48
49
50
51
52
53
54
55
56
57
58
59
60

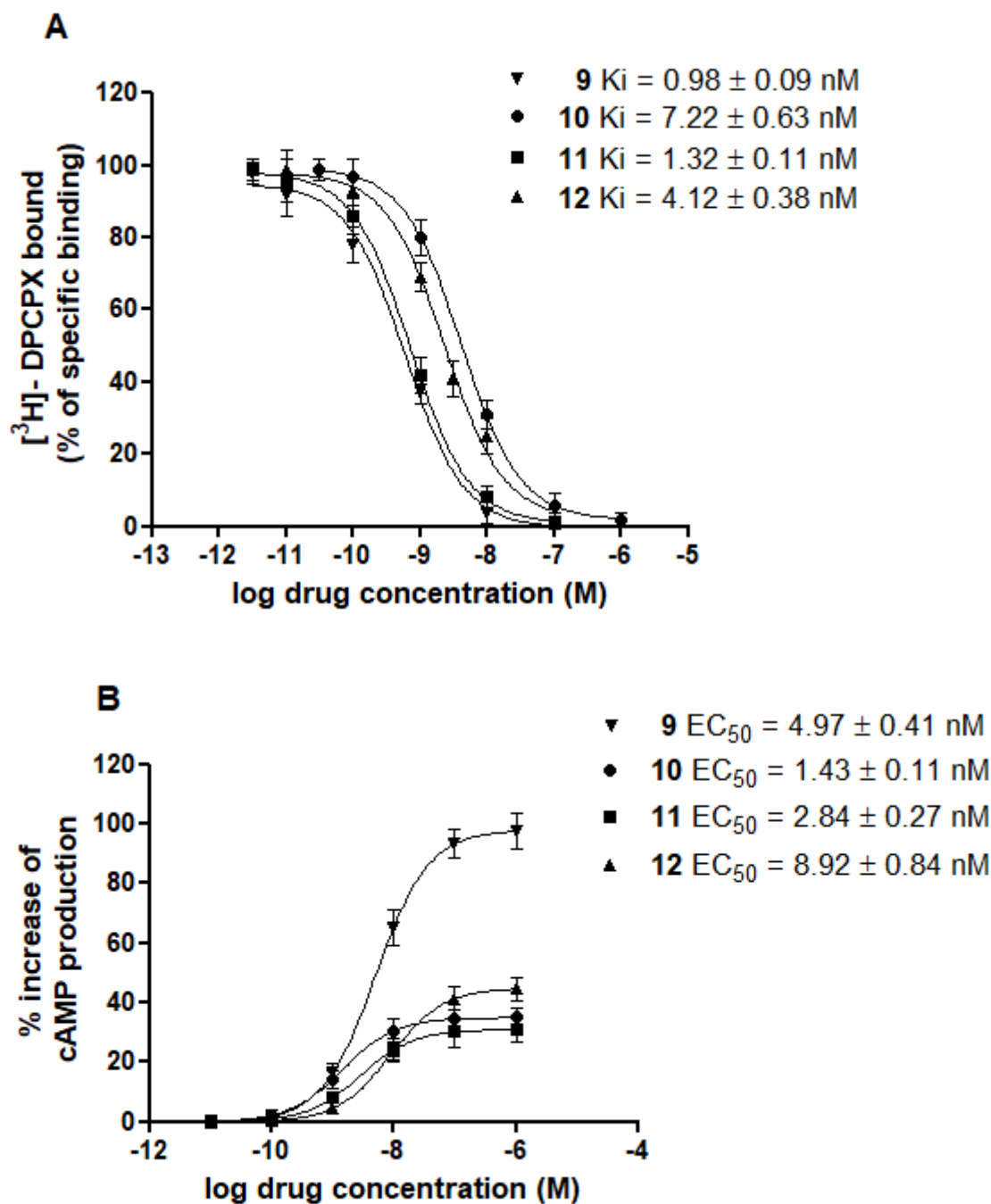
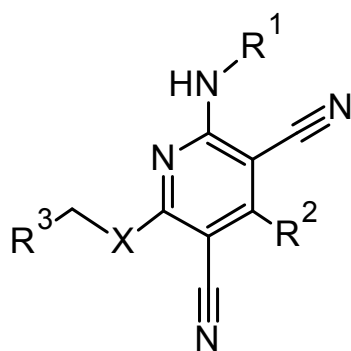
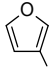
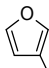
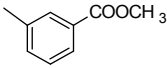
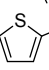
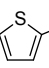
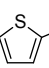
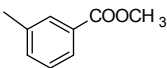
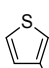
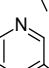
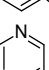
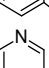
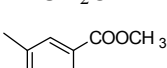
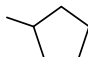
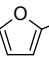
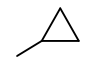
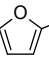
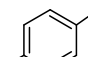
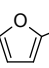
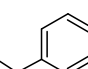
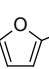
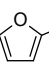


Figure 1. Competition curves of specific $[^3\text{H}]\text{-DPCPX}$ binding to $hA_1\text{ARs}$ of compounds **9-12** (A). Increase of forskolin-stimulated cAMP levels in $hA_1\text{AR}$ CHO cells by compounds **9-12** relative to the effect of DPCPX set at 100% (B). Data represent means \pm SEM of four experiments each performed in triplicate.

Table 1. Binding Affinities (K_i) at hA₁, hA_{2A} and hA₃ ARs and potencies (EC_{50}) at hA_{2B} ARs.

compd	R ¹	X	R ²	R ³	Binding experiments ^a			cAMP assays
					hA ₁ ^d	hA _{2A} ^e	hA ₃ ^f	EC ₅₀ (nM) ^b Efficacy, ^c %
1	H	S		CH ₂ OH	57±4	27%	29%	>1000 (7%)
2	H	O		CH ₂ OH	632±53	25%	3%	>1000 (11%)
3	H	NH		CH ₂ OH	20%	18%	17%	>1000 (1%)
4^g	H	S		COOCH ₃	108±9	17%	25%	>1000 (4%)
5^h	H	S		CONH ₂	175±12	21%	177±15	>1000 (17%)
6	H	S		CN	93 ± 8	887 ± 84	582 ± 56	>1000 (1%)
7^g	H	S		COOCH ₂ Ph	86±7	8%	1%	>1000 (10%)
8^h	H	S		COPh	23±2	224±21	26%	>1000 (1%)
9	H	S			0.98±0.09	31±3	25%	>1000 (4%)
10	H	S			7.22±0.63	68±3	26%	>1000 (7%)
11	H	S			1.32±0.11	67±6	326±31	>1000 (6%)
12	H	S			4.12±0.38	581±54	611±58	>1000 (1%)
13	H	S			1.02±0.11	93±9	668±64	>1000 (7%)
14	H	S			82±8	1%	11%	>1000 (7%)
15	H	S			40 ± 3	114±10	678 ± 62	>1000 (14%)
16	H	S			1.42±0.15	24±3	948±82	>1000 (1%)
17	H	S			2.71±0.21	108±9	134±12	>1000 (9%)

18	H	S		CH ₂ OH	19 ± 2	19%	34%	852 ± 81 (32%)
19	H	S			2.11±0.19	96±8	1%	>1000 (7%)
20 ⁱ	H	S		CH ₂ OH	52 ± 5	1%	554 ± 52	885± 79 (69%)
21 ⁱ	H	NH		CH ₂ OH	324 ± 28	33%	29%	>1000 (1%)
22	H	S			2.72±0.21	693 ± 68	15%	982±95 (62%)
23	H	S		CH ₂ OH	60 ± 6	9%	33%	>1000 (8%)
24	H	S		CH ₂ OH	35 ± 2	7%	22%	>1000 (18%)
25	H	NH		CH ₂ OH	1%	1%	8%	>1000 (1%)
26	H	S			1.18±0.11	636±57	8%	>1000 (15%)
27		S		CH ₂ OH	742 ± 68	8%	780 ± 72	>1000 (1%)
28		S		CH ₂ OH	89±7	30%	30%	>1000 (4%)
29		S		CH ₂ OH	10%	1%	8%	>1000 (1%)
30		S		CH ₂ OH	65±6	461±42	14%	>1000 (3%)
31	COCH ₃	S		CH ₂ OH	243±21	11%	211±18	>1000 (3%)
DPCPX					1.09±0.07	97±8	985±92	>1000 (1%)

^a K_i values are means ± SEM of four separate assays, each performed in triplicate. Percentage of inhibition (I%) of specific binding at 1 μM concentration.

^b EC₅₀ values are means ± SEM of four separate assays, each performed in triplicate.

^c Efficacy at 1 μM concentration, in comparison with NECA (1 μM = 100%).

^d Displacement of specific [³H]DPCPX binding at hA₁ARs expressed in hA₁CHO cells.

^e Displacement of specific [³H]ZM241385 binding at hA_{2A}ARs expressed in hA_{2A}CHO cells.

^f Displacement of specific [¹²⁵I]AB-MECA binding at hA₃ARs expressed in hA₃CHO cells.

^g Reference 43.

^h Reference 44.

ⁱ Reference 45.

Table 2. Potency at hA_{2B} ARs of selected amino-3,5-dicyanopyridine derivatives in the cAMP assay in CHO cells.^a

compd	IC ₅₀ (nM) ^b
	or I% ^c
1	33%
3	6%
9	152 ± 13
10	25%
11	13 ± 1
12	12%
15	40%
18	38%
21	4%
DPCPX	43 ± 4

^acAMP experiments in hA_{2B} CHO cells stimulated by 100 nM NECA (EC₅₀ = 125 ± 15 nM).^b Potency values (IC₅₀) are expressed as means ± SEM of four independent cAMP experiments, each performed in triplicate. ^cPercentage of inhibition (I%) is determined at 1 μM concentration of the tested compound.

Table 3. Modulation of Forskolin-stimulated cAMP levels of selected amino-3,5-dicyanopyridine derivatives on cyclic cAMP assay in hA₁ CHO cells.^a

compd	EC ₅₀ (nM) ^b	E _{max} (%) ^c	compd	EC ₅₀ (nM) ^b	E _{max} (%) ^c
1	128 ± 11	83 ± 6	17	3.41 ± 0.32	30 ± 4
7	192 ± 17	53 ± 5	18	58 ± 5	39 ± 5
8	57 ± 4	29 ± 3	19	4.35 ± 0.38	51 ± 5
9	4.97 ± 0.41	98 ± 7	20	107 ± 9	74 ± 6
10	1.43 ± 0.11	35 ± 4	22	3.85 ± 0.31	56 ± 6
11	2.84 ± 0.27	31 ± 3	23	142 ± 12	62 ± 4
12	8.92 ± 0.84	45 ± 4	24	94 ± 8	75 ± 5
13	4.82 ± 0.39	100 ± 8	26	6.26 ± 0.58	72 ± 6
14	185 ± 16	24 ± 3	DPCPX	1.52 ± 0.12	100 ± 9
16	2.73 ± 0.21	47 ± 5			

^aPotency values (EC₅₀) are expressed as means ± SEM of four independent cAMP experiments, each performed in triplicate. The compounds have been tested on Forskolin at 5 μM concentration.

^bPotency of the novel compounds to increase Forskolin-stimulated cAMP levels. ^cEfficacy (E_{max}) of the novel compounds were normalized by using the E_{max} of the reference compound DPCPX (set at 100%) that showed the higher capability to increase cAMP production.

Table 4. Potencies at hA_{2A}AR of selected amino-3,5-dicyanopyridine derivatives in the cAMP assay in CHO cells.

compd	IC ₅₀ (nM) ^a
9	22 ± 2
10	313 ± 29
11	58 ± 5
16	83 ± 7
DPCPX	132 ± 14

^aPotency values (IC₅₀) of selected compounds to counteract the CGS 21680-stimulated cAMP levels in hA_{2A}CHO cells. IC₅₀ values are expressed as means ± SEM of four independent cAMP experiments, each performed in triplicate.

Introduction at R³ position of small non-aromatic side chains yielded derivatives **1-6** that preferentially bind the hA₁AR. Hence, the presence of a phenyl moiety on the R³ substituent (compounds **7, 8**) maintained the hA₁AR affinity in the nanomolar range, but also the interaction with the hA_{2A} receptor was implemented (see compound **8**). Aryl homologation of derivatives **1** and **4-6** produced a high increase of hA₁AR affinity yielding derivatives **9-11, 13**, all active in the low nanomolar range. Also a substantial improvement of hA_{2A} receptor-ligand interaction was observed. This behavior was expected considering that these modifications lead to an increased lipophilicity of the R³ substituent while its hydrogen bonding properties were maintained. Transformation of the carboxymethyl function of **10** into the corresponding acid **12** maintained the hA₁AR affinity but reduced the hA_{2A} binding. Isosteric replacement of the phenyl moiety at the R³ position of **10** with a furan ring yielded compound **14** which is endowed with good hA₁AR affinity and high selectivity versus the other hARs. To evaluate the effect of other heteroaryl moieties at R³ position, 2-, 3- and 4-pyridinyl groups were introduced yielding compounds **15-17** that showed from high to good hA₁ and hA_{2A} AR affinity. The hA₃ receptor binding data of the aminopyridines discussed till now seem to be influenced by the aromatic nature of the R³ substituent. In fact, compounds **11-13** and **15-17** recovered some affinity for this receptor subtype, the best being compound **17**. Furthermore, modifications at

1
2
3 R² were performed by replacing the 2-furanyl moiety with a 3-furanyl, 2- and 3-thienyl and 3-
4 pyridinyl group in order to understand how the different heterocyclic substituents could modulate AR
5 binding affinity, selectivity and pharmacological profile of the target compounds. At a glance, these
6 binding data let us to hypothesize that the furan ring at R² is important for the anchoring of these
7 aminopyridine derivatives at the hA_{2A} subtype. In fact, by comparing hA_{2A} K_i values of the 2- and 3-
8 furanyl derivatives **10** and **19** with the corresponding 4-(2-thienyl) and 4-(3-pyridinyl) compounds
9 **22** and **26**, respectively, it emerged that the hA_{2A} binding affinity was about ten-fold reduced, while
10 K_i values at hA₁AR are highly preserved in the low nanomolar range. As observed for compound **1**
11 and the other 4-(2-furanyl) derivatives bearing a non-aromatic R³ substituent (**4-6**), hA₁AR affinity
12 was preserved when other R² heteroaryl substituents are present leading also to some selective
13 compounds. Replacing the 6-thiomethyl chain of the derivatives **1**, **20** and **24** with an oxy- (compound
14 **2**) or an amino- (**3**, **21**, **25**) methyl group turned out to be detrimental for hA₁AR affinity. Finally, the
15 primary 2-amine function of **1** was hindered by insertion of various R¹ substituents to evaluate the
16 role of this position in the binding at all the hARs, especially at the hA₁ one. Cycloalkyl groups
17 (compounds **27**, **28**) or other moieties (**29-31**) that were reported to ameliorate affinity and/or
18 selectivity toward a specific hAR subtype have been taken into consideration.⁶ In particular, this
19 information could be important to understand the binding mode of these amino-3,5-dicyanopyridine
20 derivatives at the hA₁ subtype. Not expected was the 13-fold lower hA₁ binding affinity of the 2-
21 (cyclopenthyl)amino derivative **27** with respect to the 2-amino analogue **1**. Moreover, while
22 compounds **28** and **30** bind the hA₁AR as the lead **1**, the 6-(4-iodophenyl)amino derivative **29** did not
23 show any affinity for any hARs.

24
25
26
27
28
29
30
31
32
33
34
35
36
37
38
39
40
41
42
43
44
45
46
47
48
49
50
51
52 In contrast, the presence of a 2-(N-acetylamino) group (compound **31**) enhances the hA₃AR affinity
53 suggesting that an acyl moiety at this position could be useful for shifting the binding of the amino-
54 3,5-dicyanopyridines toward the hA₃AR, as extensively demonstrated for other hAR ligands in the
55 literature.^{6,27,55}
56
57
58
59
60

Molecular Modeling Studies

Molecular docking studies were carried out at the hA₁AR 3D structure to analyze the binding data of the developed compounds. We employed the crystal structure of the hA₁AR bound to the xanthine-based ligand 4-[3-(8-cyclohexyl-2,6-dioxo-1-propyl-7H-purin-3-yl)propylcarbamoyl]benzenesulfonyl fluoride (DU172) (<http://www.rcsb.org>; pdb code: 5UEN; 3.2-Å resolution⁵⁶). The crystal structure was refined within MOE⁵⁷ software and prepared for docking experiments. Docking analyses were performed with CCDC Gold⁵⁸ and Autodock software (within PyRx interface).⁵⁹⁻⁶¹ Analogous studies for a subset of compounds were performed even at the crystal structure of the hA_{2A}AR in complex with the inverse agonist 4-(-2-(7-amino-2-(2-furyl)[1,2,4]triazolo[2,3-a][1,3,5]triazin-5-yl-amino)ethyl)phenol (ZM241385) (pdb code: 4EIY; 1.8-Å resolution⁶²) and at a homology model of the hA₃AR. The binding mode corresponding to the best score generally presents the compounds of interest oriented analogously to the structurally related non-nucleoside agonists docked at other AR subtypes (Figure 2A).^{63,64} In detail, the pyridine scaffold gets located in the hA₁AR cavity in correspondence with the xanthine core of DU172 observed from the hA₁AR crystal structure, between the side chains of Phe171 (EL2), Leu250^{6,51}, and Ile274^{7,39}. For clarity, in this section, derivative **9** has been considered as the reference compound to define the position of the substituents on the pyridine nucleus. Thus, starting from the N1 position, the amino and the sulfanyl functions occupy positions 2 and 6, respectively. In general, the exocyclic amino group at the 2-position and the 3-cyano group make a double H-bond interaction with the side chain of Asn254^{6,55}, while the 5-cyano group points toward the region between Ala66^{2,61}, Ile274^{7,39}, and His278^{7,43} (Figure 2B).

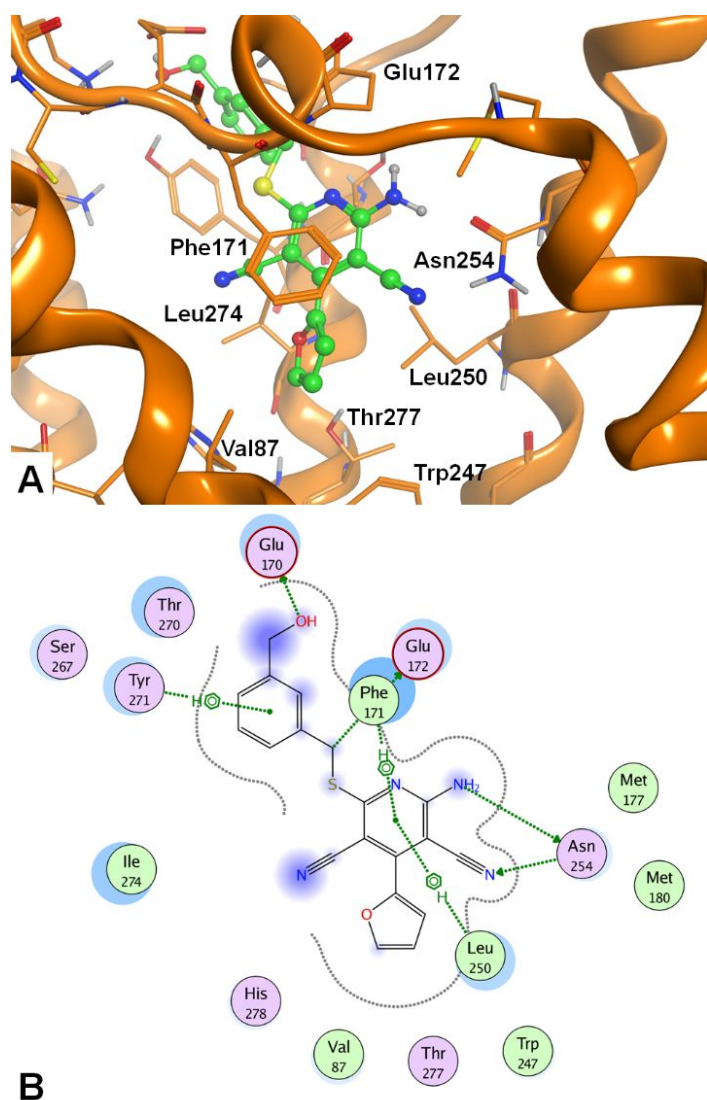


Figure 2. A. Docking conformations of the synthesized compounds at the hA₁AR (PDB: 5UEN⁵⁶) cavity, taking **9** as template. Key receptor amino acids are indicated. B. Schematic view of the compound-receptor interaction (developed with the Ligand Interaction tool within MOE).

The 6-substituent is oriented toward the entrance of the binding cavity (Figure 3), modulating the interaction with the receptor. Docking results show that the 6-arylalkylthio chain does not remain coplanar with respect to the pyridine ring, as the dihedral angle between the N1 and the C6 atoms, and the S-CH₂ linking group on the 6-substituent results about 60° for most of the compounds. This may be allowed for a thiomethyl- or oxymethyl-containing chain but it gets associated to a much higher

energy when the linker is an amino group due to conjugation effects. Accordingly, binding data show that the hA₁ binding affinity decreases when in the 6-position analogous thiomethyl- or oxymethyl-containing chains are replaced by the corresponding amino-based substituents (i.e. compare compounds **1**, **2** and **3**, respectively). Furthermore, the 6-heteroatom gets located near hydrophobic residues like Ile274^{7,39}; this may explain while the sulphur-based chains lead to a higher hA₁ affinity with respect to the corresponding oxygen-based substituents, which are characterized by higher polarity.

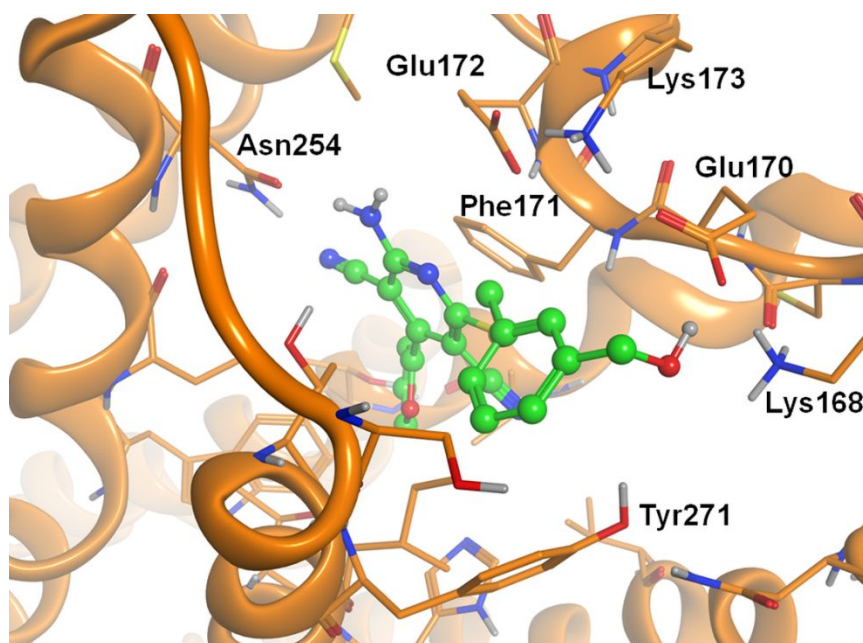


Figure 3. Top-view of the docking conformations of the synthesized compounds at the hA₁AR (PDB: 5UEN⁵⁶) binding site, taking **9** as example: detailed view of the interaction between the 6-substituent and the receptor aminoacids at the entrance of the binding cavity.

In general, compounds bearing a R³ substituent that contains an aromatic ring functionalized with a polar function (i.e. compounds **9-13** and **15-17**) are endowed with the highest affinity at the hA₁AR. As shown in Figure 3 for compound **9**, this polar group (the hydroxymethyl in this case) makes interactions with polar residues which are present at the entrance of the binding cavity. In fact, the

1
2
3 presence of polar groups bearing H-bond acceptor or donor functions makes it possible to give
4 interaction with polar amino acids such as Ser267^{7,32} or with both positively or negatively charged
5 residues such as Lys168 and Glu170 (both belonging to the EL2 segment), gaining in both cases a
6 good affinity for the hA₁ receptor. In particular, the presence of a polar group at the meta-position of
7 the aromatic R³ ring allows the polar function to interact with polar residues in the binding pocket,
8 considering various orientations of the aromatic ring. Even when the R³ substituent is a nitrogen-
9 containing heterocycle such as the pyridyl ring, the highest affinity is obtained with the polar nitrogen
10 atom inserted at the meta-position of the ring itself (compare the hA₁AR affinity of **15**, **16**, and **17**).
11
12 The 4-heterocyclic substituent is inserted in the depth of the cavity, close to residues belonging to
13 TM3, EL2, TM6, and TM7 domains (Val87^{3,32}, Phe171, Trp247^{6,48}, Leu250^{6,51}, Ile274^{7,39}, Thr277^{7,42},
14 and His278^{7,43}). The chemical-physical profile of the ring appears to modulate the affinity for the
15 hA₁AR. The affinity data reported in Table 1 indicate that a 4-heterocycle bearing a polar atom at the
16 3-endocyclic position appears to be more beneficial for the hA₁AR binding affinity with respect to
17 both a 4-heterocycle containing polar atom at the 2-endocyclic position and a non-polar 4-substituent
18 (considering sets of compounds presenting the same 6-substituent). We analysed these data with the
19 *IF-E 6.0* tool, to calculate the per-residue interaction energies (expressed as kcal mol⁻¹; see
20 Experimental section for details). This tool was previously used for analogue analyses at hARs
21 obtaining useful interpretation of the compound activity.^{29,34,42,63,65} We considered two sets of
22 compounds that differed only in terms of the 4-heterocycle (first set: **10**, **19**, **22**, and **26**; second set:
23 **1**, **18**, **20**, **23**, and **24**). The results are displayed in Figure 4.
24
25
26
27
28
29
30
31
32
33
34
35
36
37
38
39
40
41
42
43
44
45
46
47
48
49
50
51
52
53
54
55
56
57
58
59
60

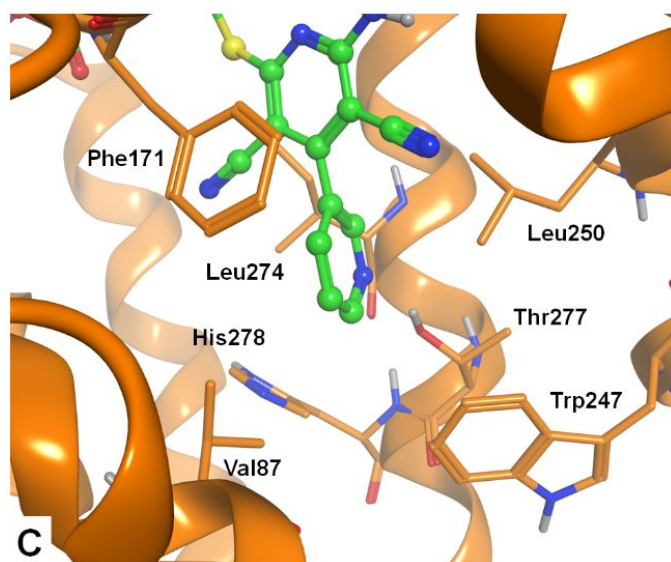
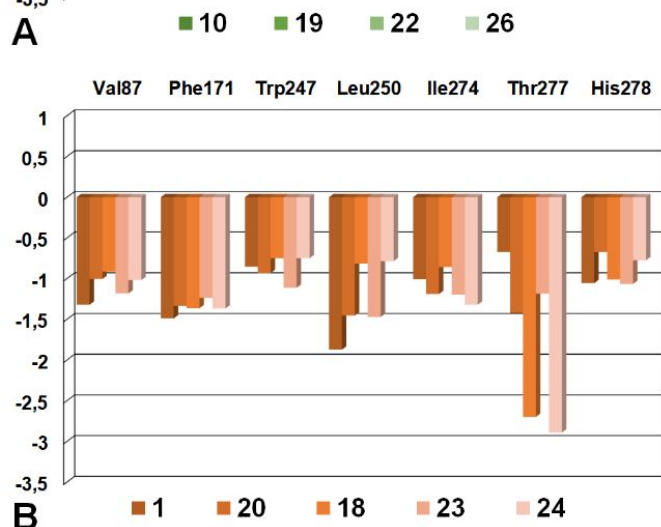
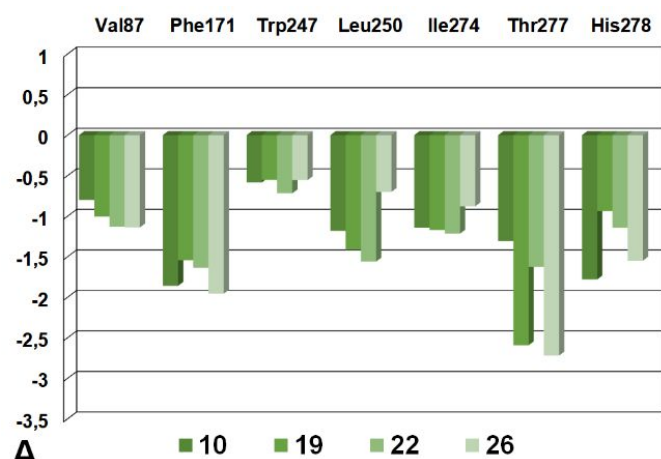


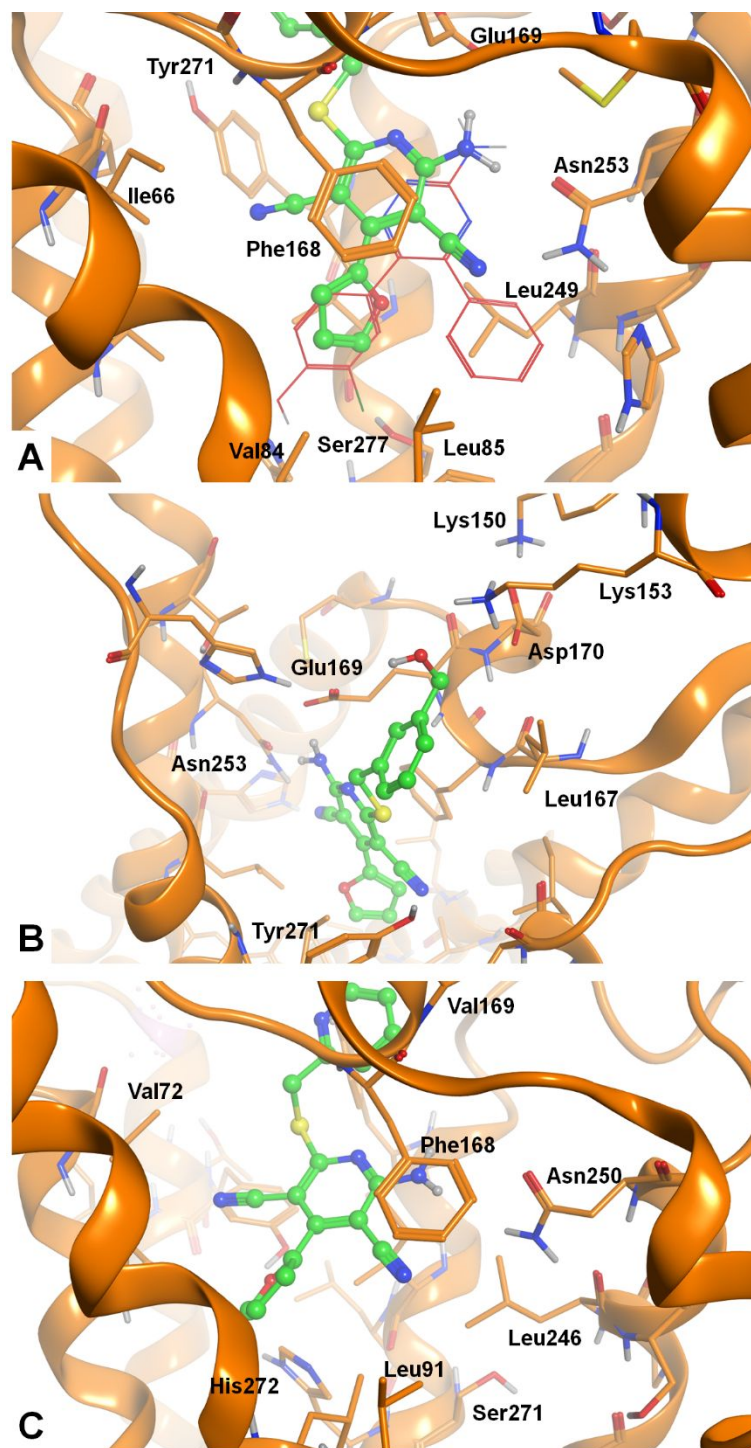
Figure 4. A-B. Ligand-target interaction energies calculated with the *IF-E 6.0* tool within MOE (see text for details) for sets of compounds differing only based on the 4-substituent. The receptor's amino acids located close to the 4-substituent were considered and are displayed in panel C. Data are represented as kcal mol⁻¹. The results show a significant interaction with Thr277^{7,42} for residues

1
2
3 presenting a polar atom at the 3-endocyclic position within the 4-substituent (i.e. **19** and **26** in the first
4 set and **18** and **24** in the second set). C. Detail of the ligand-target interaction at the 4-substituent
5 (compound **26** is shown in this figure). The key residues (PDB: 5UEN⁵⁶) involved in this interaction
6 are displayed and indicated.
7
8
9
10

11
12
13
14 It may be observed that the compounds presenting a 4-heterocycle containing a polar atom at the 3-
15 endocyclic position have higher interaction with the Thr277^{7,42} residue with respect to the other
16 analogues (i.e. **19** and **26** vs **22** and **10**, or **18**, **24** and **23** vs **1** and **20**). The interaction of the 4-moiety
17 with the residues in its proximity presents analogous trends within each set of compounds. Figure 4
18 shows the general position of the 4-substituent within the binding cavity and the residues present in
19 its proximity. Among the various residues, the 3-position of the 4-heterocycle moves in proximity to
20 the hydroxyl group of the Thr277^{7,42} sidechain.
21
22
23
24
25
26
27
28
29

30 Docking experiments were performed also at the hA_{2A}AR crystal structure and at a hA₃AR homology
31 model with the same protocol used at the hA₁AR. Compounds endowed with affinity for these
32 receptor subtypes were considered in this task. Docking results at the hA_{2A}AR show an analogue
33 binding mode of the analysed compound **9** at the receptor cavity with respect to the docking
34 conformations at the hA₁AR (Figure 5 shows an hA_{2A}AR-compound **9** complex as example).
35 Analogous considerations made for the 6-substituent at the hA₁AR may be applied at the hA_{2A}AR
36 and this may be due to the presence in the hA_{2A}AR of residues having analogous position and
37 chemical-physical profile with respect to the hA₁AR amino acids interacting with the 6-substituent
38 (i.e. Lys153, Glu169, and Asp170 in hA_{2A}AR compared to Lys168, Glu170, and Glu172 in hA₁AR;
39 Figure 5B). Even the affinity trend is conserved as the most potent compounds at the A₁AR are
40 endowed with the highest hA_{2A}AR affinity, even if the activity at the latter receptor is generally lower.
41
42
43
44
45
46
47
48
49
50
51
52
53
54
55
56
57
58
59
60
60 Higher hA₁AR selectivity is observed based on the kind of heterocycle inserted at the 4-position,
where the presence of a thienyl or a pyridyl group leads to a significant decrease of the hA_{2A}AR
affinity with respect to the furanyl moiety. Figure 5A shows that the position of the 4-heterocycle

1
2
3 corresponds to the one of the 2-chlorophenol substituent of the 3-amino-1,2,4-triazine derivative co-
4
5 crystallized with the hA_{2A}AR (pdb code: 3UZC).⁶⁶
6
7
8
9
10



58 **Figure 5.** A. Docking conformations of the synthesized compounds at the hA_{2A}AR cavity, taking
59 compound **9** (green) as template. Key receptor amino acids are indicated. The position of the 4-
60

1
2
3 heterocycle corresponds to the one of the 2-chlorophenol substituent of the 3-amino-1,2,4-triazine
4 derivative (red) co-crystallized with the hA_{2A}AR (pdb code: 3UZC⁶⁶). **B.** Top-view of the docking
5
6 conformations of the synthesized compounds at the A₁AR cavity, taking compound **9** as example:
7
8 detailed view of the interaction between the 6-substituent and the receptor aminoacids at the entrance
9
10 of the binding cavity. **C.** Binding mode of compound **17** at the hA₃AR cavity, analogue to the top-
11
12 score docking conformations at the hA₁AR and hA_{2A}AR. Key receptor residues are indicated. This
13
14 binding mode was observed only for some of the analyzed derivatives at the hA₃AR cavity.
15
16
17
18
19
20

21
22 Docking results at a hA₃AR homology model showed different behavior of the analyzed molecules
23
24 at the binding cavity and a conserved binding mode for these molecules could not be depicted. The
25
26 above described binding mode was observed only for a few molecules at this receptor cavity (Figure
27
28 5C). The top-score docking conformations make the compounds generally located more externally
29
30 respect to the other hAR cavities. The lack of positively or negatively charged residues in proximity
31
32 to the 6-substituent (with respect to that observed at the other hARs) could have a role in stabilizing
33
34 the compounds in a slightly displaced position with respect to the hA₁ and hA_{2A} ARs, with a
35
36 consequent loss of binding interaction for several derivatives that are able to still bind the hA_{2A}AR
37
38 even if with lower affinity than the hA₁AR.
39
40
41

42
43 Docking results at the hA₁AR presented the 2-amino function of these compounds as being located
44
45 almost in correspondence to the 6-amine of Ado/NECA compounds co-crystallized with the
46
47 hA_{2A}AR.⁶⁷ Given that some reference A₁AR agonists were obtained by inserting cycloalkyl groups
48
49 at the N⁶-position of Ado (i.e. N⁶-cyclopentyladenosine or CPA) and in general the presence of alkyl
50
51 or cycloalkyl groups led to an improvement of the hA₁AR affinity, we have modified compound **1** by
52
53 inserting an alkyl/cycloalkyl/arylalkyl substituent on the 2-amino group. As reported in Table 1,
54
55 differently from what was expected, this modification did not produce an improvement of the hA₁AR
56
57 affinity, leading to a significant decrease in some cases. Docking results of these compounds at the
58
59 hA₁AR showed that the presence of a substituted 2-amino group led the compounds to be oriented in
60

1
2
3 the pocket in several ways, but not in the above-described conformation which is adopted by the 2-
4 unsubstituted molecules (i.e. compound **1** itself). Also, a preferred arrangement for this set of
5
6 compounds could not be depicted.
7
8
9

10 11 12 13 **Behavioral studies in the oxaliplatin-induced neuropathy model**

14
15 It has been reported that non-selective blockade of ARs exerted by caffeine, especially of A₁ and A_{2A}
16 subtypes, could be related to its well-known neuroprotective effects.^{11,13,21} In light of this hypothesis,
17
18 four selected compounds, **9-12**, were studied in an *in vivo* mouse model of oxaliplatin-induced
19 neuropathy. In particular, the pain relieving effect induced by a single oral (*per os*, p.o.)
20 administration of different doses of these compounds was evaluated. The pain threshold of mice,
21 evaluated as hypersensitivity to a cold, non-noxious, stimulus (allodynia-like measurements; Cold
22 plate test)⁶⁸ was progressively reduced by a daily treatment with oxaliplatin (2.4 mg kg⁻¹
23 intraperitoneally - ip). On day 15, licking latency dropped to 10.8 ± 0.8 s when compared to that of
24 control mice (18.5 ± 1.5 s) treated with the vehicle (Figure 6). The acute administration of compound
25
26 **9** was able to elicit a significant increase of the licking latency, starting from 0.01 mg kg⁻¹. The higher
27 doses, 0.1 and 0.3 mg kg⁻¹, induced progressively enhanced effects, reaching a complete reversion of
28 hypersensitivity between 15 and 45 min after administration. Similarly, **10** (0.1 and 0.3 mg kg⁻¹)
29 evoked full pain relief; the onset was at 15 min, peaking between 30 and 45 min. Compound **11** was
30 effective when 1 mg kg⁻¹ was administered, whereas the lower dose (0.3) was inactive. In comparison,
31
32 **12** was more potent than **11**, even if the onset was delayed by 30 min (Figure 6).
33
34
35
36
37
38
39
40
41
42
43
44
45
46
47
48
49

50 All these compounds showed the characteristic profile of inverse agonist of the A₁ receptor and
51 antagonist for the A_{2A} subtype. The pharmacodynamic possibility to negatively modulate both the A₁
52 and A_{2A} receptor subtypes suggests analogies with caffeine. Several biological effects of the natural
53 xanthine are mediated by the antagonism to the adenosine receptors.⁶⁹ Caffeine-dependent
54
55
56
57
58
59
60

antinnocption can be attributed to the blockade of the hA_{2A} ,²⁴ and the A_1 ⁷³ subtypes suggesting the relevance of both these mechanisms in the efficacy of our compounds.

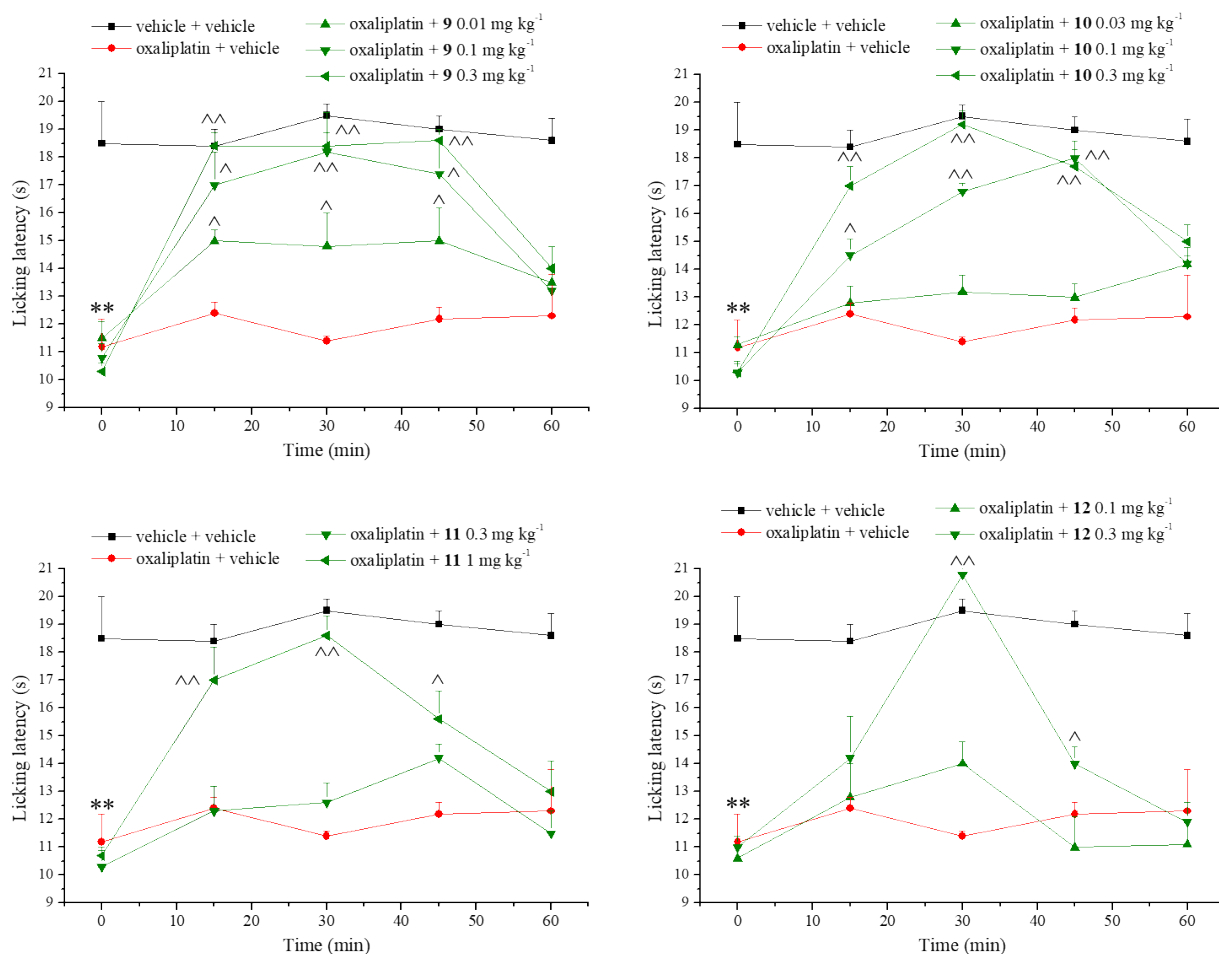


Figure 6. Effects of selected compounds against neuropathic pain in mice. Neuropathy was induced by repeated i.p. injection of oxaliplatin (2.4 mg kg^{-1} , daily). The hypersensitivity to a cold thermal stimulus was measured on day 15 by the Cold plate test (latency to pain related behaviors as paw lifting or licking). Compounds **9-12** were administered p.o, measurements were performed 15, 30, 45, and 60 min after. Control mice were treated with vehicle. Each value represents the mean of 10 mice per group, performed in 2 different experimental sets. ** $P < 0.01$ vs vehicle + vehicle treated mice. ^ $P < 0.05$ and ^^ $P < 0.01$ vs oxaliplatin + vehicle treated mice.

1
2
3 To validate the hypothesis of similarity, caffeine (10 mg kg⁻¹ p.o.) was also tested and a significant
4 decrease of oxaliplatin-mediated hypersensitivity was generated (Figure 7). It is worth noting that
5
6
7 both A₁ and A_{2A} receptors have presynaptic and postsynaptic location; acting at presynaptic
8
9
10 heteroreceptors they may modulate neurotransmitter release from dopamine, serotonin^{70,71} and
11
12 acetylcholine (ACh) terminals.⁷² In particular, caffeine, via blockade of inhibitory presynaptic
13
14 adenosine receptors, was able to induce a central cholinergic analgesia by ACh increase.⁷³ The present
15
16 results show, for the first time, that the efficacy of caffeine against neuropathic pain is mediated by
17
18 the cholinergic system. In accordance with previous results that individuated the main relevance of
19
20 cholinergic signaling in neuropathic condition in the nicotinic component,⁷⁴ the caffeine effect was
21
22 blocked by the non-specific nAChR (nicotinic ACh receptor) antagonist mecamylamine (meca;
23
24 Figure 7). More specifically, caffeine reduced oxaliplatin-induced pain by a mechanism involving the
25
26 alpha7 subtype of nAChRs in accordance with previously published data about the role of alpha7
27
28 nAChR in chemotherapy-induced neuropathy,⁷⁵ since its activity was lost in the presence of the
29
30 selective alpha7 nAChR antagonist methyllycaconitine (MLA).
31
32
33

34
35 Following this reasoning, we hypothesized a similar mechanism for the new synthesized compounds.
36
37 The effect of nAChR antagonists were tested on the particularly active compounds **9** and **10**. As
38
39 shown in Figures 8 and 9, the anti-neuropathic effect of **9** and **10** were completely blocked by both
40
41 meca and MLA. Involvement of the positive modulation of alpha7 nAChR in the pharmacodynamic
42
43 mechanism of the new derivatives is proposed.
44
45
46
47
48
49
50
51
52
53
54
55
56
57
58
59
60

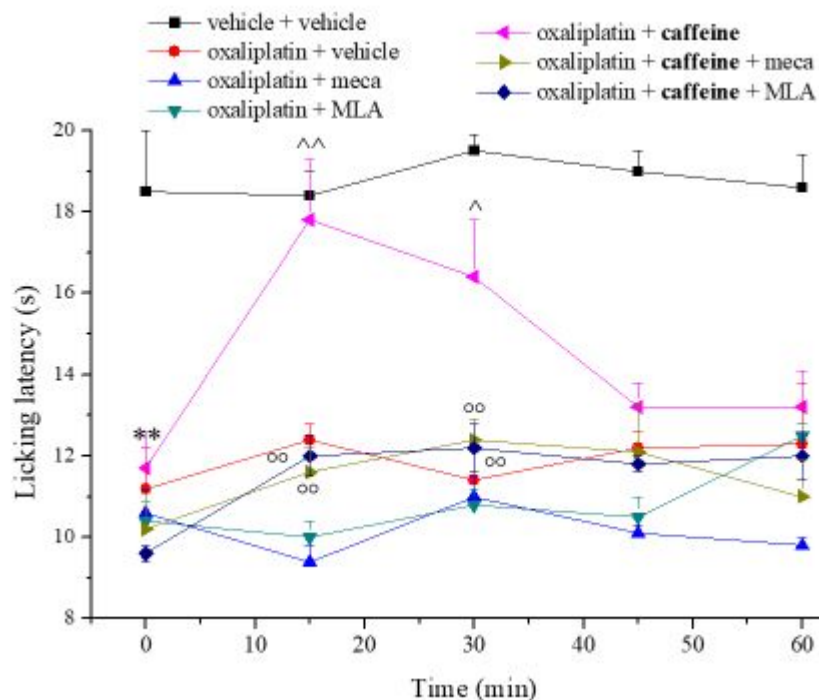


Figure 7. Effects of caffeine against neuropathic pain in mice. Role of nAChRs. Neuropathy was induced by repeated i.p. injection of oxaliplatin (2.4 mg kg^{-1} , daily). The hypersensitivity to a cold thermal stimulus was measured on day 15 by the Cold plate test (latency to pain related behaviors as paw lifting or licking). Caffeine was administered p.o. at 10 mg kg^{-1} . The non-selective nAChR antagonist mecamylamine (meca; 2 mg kg^{-1} i.p.) and the selective $\alpha 7$ nAChR antagonist methyllycaconitine (MLA; 6 mg kg^{-1} i.p.) were administered 15 min before caffeine. Measurements were performed overtime after the injection of caffeine or vehicle (in control mice). Values are reported as mean of 10 mice per group (two different experimental sets). $**P < 0.01$ vs vehicle + vehicle treated mice. $^{\wedge}P < 0.05$ and $^{\wedge\wedge}P < 0.01$ vs oxaliplatin + vehicle treated mice. $^{\circ\circ}P < 0.01$ vs oxaliplatin + caffeine treated mice.

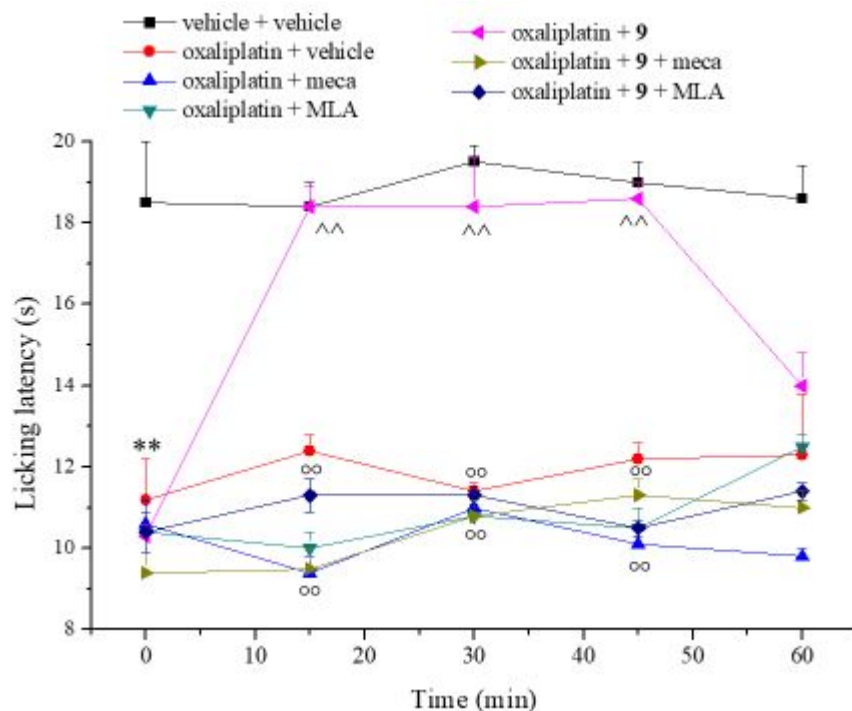


Figure 8. Effects of nicotinic antagonisms on compound **9** anti-hyperalgesic efficacy. Neuropathy was induced by repeated i.p. injection of oxaliplatin (2.4 mg kg^{-1} , daily). The hypersensitivity to a cold thermal stimulus was measured on day 15 by the Cold plate test (latency to pain related behaviors as paw lifting or licking). The non-selective nAChR antagonist mecamylamine (meca; 2 mg kg^{-1} i.p.) and the selective $\alpha 7$ nAChR antagonist methyllycaconitine (MLA; 6 mg kg^{-1} i.p.) were administered 15 min before **9** (0.3 mg kg^{-1} p.o.). Measurements were performed overtime after the injection of **9** or vehicle (in control mice). Values are reported as mean of 10 mice per group (two different experimental sets). ** $P < 0.01$ vs vehicle + vehicle treated mice. $\wedge P < 0.05$ and $\wedge\wedge P < 0.01$ vs oxaliplatin + vehicle treated mice. $\circ P < 0.01$ vs oxaliplatin + **9** treated mice.

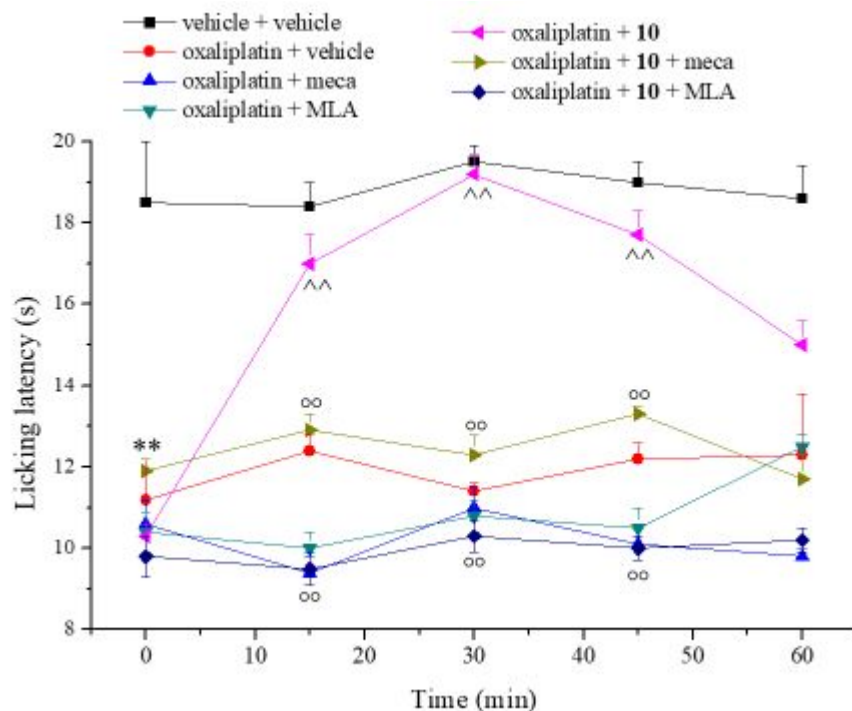


Figure 9. Effects of nicotinic antagonisms on **10** anti-hyperalgesic efficacy. Neuropathy was induced by repeated i.p. injection of oxaliplatin (2.4 mg kg^{-1} , daily). The hypersensitivity to a cold thermal stimulus was measured on day 15 by the Cold plate test (latency to pain related behaviors as paw lifting or licking). The non-selective nAChR antagonist mecamylamine (meca; 2 mg kg^{-1} i.p.) and the selective $\alpha 7$ nAChR antagonist methyllycaconitine (MLA; 6 mg kg^{-1} i.p.) were administered 15 min before **10** (0.3 mg kg^{-1} p.o.). Measurements were performed overtime after the injection of **10** or vehicle (in control mice). Values are reported as mean of 10 mice per group (two different experimental sets). ** $P < 0.01$ vs vehicle + vehicle treated mice. $\wedge P < 0.05$ and $\wedge\wedge P < 0.01$ vs oxaliplatin + vehicle treated mice. $\circ\circ P < 0.01$ vs oxaliplatin + **10** treated mice.

Chemical stability study

This study was devoted to establishing the chemical stability of the carboxylate ester **10**. In fact, it is well-known that the ester group can be susceptible to hydrolysis by the plasma enzymes. Therefore, to rule out that the observed pharmacological/biological activity was related to the formation of its metabolite, a series of experiments concerning the stability of compound **10** were performed. Due to the analyte concentration levels used in the stability test, the degradation analyses were performed by the LC-MS/MS method operating in the multiple reaction monitoring (MRM) mode. The instrumental conditions are reported in the Experimental Procedures section.

Degradation profiles. The stability of compound **10** was evaluated by monitoring the variation of its concentration at different incubation times. By plotting these data (analyte concentrations vs the incubation time), its respective degradation profiles in PBS, in human and in rat plasma matrices were obtained (see Supporting Information). In order to summarize all experimental data, the half-life values of studied compounds were reported in Table 5.

Table 5. Half life ($t_{1/2}$) of studied compound in human and rat plasma samples

Compd	Human Plasma	Rat Plasma
	$t_{1/2} \pm SD$ (min.)	$t_{1/2} \pm SD$ (min.)
KEE	100 ± 12	n.d.(*)
Enalapril	n.d.(*)	22 ± 8
10	≥240	≥240

(*). n.d.: not determined.

Conclusion

The amino-3,5-dicyanopyridines reported in this study proved to be potent hA₁AR inverse agonists, some of which also endowed with good selectivity versus the other hAR subtypes. However, some derivatives (**9-12**) behave as mixed hA₁AR inverse agonist/A_{2A} and A_{2B} AR antagonists, thus

1
2
3 suggesting a similar trend as observed in caffeine, psychoactive compound present in widely
4 consumed beverages, whose neuroprotective effects are well known and ascribed to the non-selective
5 blockade of ARs. Evaluation of compounds **9-12** in mice affected by neuropathic pain confirms
6 that these compounds can act like caffeine, thus representing promising candidates for the treatment
7 of persistent pain. In particular, compounds **9-10**, similarly to caffeine, showed to reduce oxaliplatin-
8 induced neuropathy by a mechanism involving the α_7 subtype of nAChRs. Thus, for the first time
9 it has been highlighted that the efficacy of caffeine against neuropathic pain is mediated by the
10 cholinergic system. Moreover, the chemical degradation profiles of the methyl carboxylate ester **10**
11 confirm the stability of this compound at the conditions operated in the oxaliplatin-induced
12 neuropathy assay as showing high half-life values. Moreover, the similar trend obtained in both rat
13 and human plasma matrices could validate the pharmacological model used. The molecular modeling
14 studies provide an interpretation of the affinity data at the hA₁AR and suggest a possible development
15 of the aminopyridine series considering the combination of the most suitable R substituent with the
16 optimization of the chemical-physical properties of the 4-heterocycle.
17
18
19
20
21
22
23
24
25
26
27
28
29
30
31
32
33
34
35
36
37
38

39 **EXPERIMENTAL PROCEDURES**

40 **Chemistry**

41
42 The microwave-assisted syntheses were performed using an Initiator EXP Microwave Biotage
43 instrument (frequency of irradiation: 2.45 GHz). Analytical silica gel plates (Merck F254),
44 preparative silica gel plates (Merck F254, 2 mm) and silica gel 60 (Merck, 70-230 mesh) were used
45 for analytical and preparative TLC, and for column chromatography, respectively. All melting points
46 were determined on a Gallenkamp melting point apparatus and are uncorrected. Elemental analyses
47 were performed with a Flash E1112 Thermofinnigan elemental analyzer for C, H, N and the results
48 were within $\pm 0.4\%$ of the theoretical values. All final compounds revealed purity not less than 95%.
49
50 The IR spectra were recorded with a Perkin-Elmer Spectrum RX I spectrometer in Nujol mulls and
51
52
53
54
55
56
57
58
59
60

1
2
3 are expressed in cm^{-1} . NMR spectra were recorded on a Bruker Avance 400 spectrometer (400 MHz
4
5 for ^1H NMR and 100 MHz for ^{13}C NMR). The chemical shifts are reported in δ (ppm) and are relative
6
7 to the central peak of the residual non-deuterated solvent, which was CDCl_3 or DMSO-d_6 . The
8
9 following abbreviations are used: s= singlet, d= doublet, t= triplet, q= quartet, m= multiplet, br=
10
11 broad, ar= aromatic protons., ax=axial, eq=equatorial. Compounds **32**, **34-36**, **37**, **39-41** were
12
13 synthesized following reported procedures.⁴⁶⁻⁵¹
14
15
16
17
18

19 **Procedure A: Synthesis of the target compounds 1, 4, 6-20, 22-24, 26.** Sodium hydrogen carbonate
20
21 (2 mmol) and the commercially available halomethyl-derivative (1 mmol) were added to a solution
22
23 of the suitable mercapto-compound (**37-41**,⁴⁹⁻⁵¹ 1 mmol) in anhydrous DMF (1 mL). The reaction
24
25 mixture was stirred at rt until disappearance of the starting material (TLC monitoring). Then, water
26
27 was added (25 mL) to precipitate a solid which was collected by filtration and washed with water.
28
29 The crude product was triturated with Et_2O (5 mL), collected by filtration and purified by
30
31 crystallization.
32
33
34
35
36

37 **Procedure B: Synthesis of compound 2.** A mixture of compound **43**⁵³ (0.53 mmol), 2-bromoethanol
38
39 (0.58 mmol) and sodium hydrogen carbonate (0.79 mmol) in dry DMF (1 mL) was heated at 80°C
40
41 under microwave irradiation for 3 h. Then, water (30 mL) was added and the mixture was extracted
42
43 with CH_2Cl_2 (3x25 ml). The collected organic layers were washed with brine (2x20 mL), dried
44
45 (Na_2SO_4) and evaporated under reduced pressure to yield a pale green solid that was purified by
46
47 preparative TLC on silica gel, using $\text{CH}_2\text{Cl}_2/\text{MeOH}$ 9:1 as eluent and then recrystallized.
48
49
50
51
52

53 **Procedure C: Synthesis of 4-substituted-2-amino-6-((2-hydroxyethyl)amino)pyridine-3,5-**
54
55 **dicarbonitriles 3, 21, 25.** A solution of the suitable phenylsulfanyl-derivative **32**⁴⁶, **34**⁴⁶, **36**⁴⁸ (0.5
56
57 mmol) and 2-aminoethanol (2 mmol) in DMF (2 mL) was heated at 100°C until the disappearance of
58
59 the starting material (TLC monitoring: silica gel, $\text{CHCl}_3/\text{MeOH}$ 9:1). After cooling at rt, water (10
60

mL) was added and the resulting precipitate was collected by filtration and washed with water (10 mL) and Et₂O (5 mL).

Procedure D: Synthesis of compound 5.⁴⁴ An aqueous solution of KOH (10%, 0.28 mL) was added to a suspension of compound **37**⁴⁹ (0.5 mmol) in DMF (2 mL). The reaction mixture was stirred at rt for 5 min and then, chloroacetamide (1 mmol) was added. After stirring at rt for 5h, water (10 mL) was added and the resulting suspension was extracted with EtOAc (3x10 mL). The collected organic layers were dried (Na₂SO₄) and the solvent removed under reduced pressure, yielding the crude product which was triturated with Et₂O (2 ml) and collected by filtration.

Procedure E: Synthesis of 2-amino-substituted 4-(furan-2-yl)-6-((2-hydroxyethyl)sulfanyl)pyridine-3,5-dicarbonitriles 27-30. An excess of the suitable primary amine (2.0 mmol) was added to a solution of **44** (1.0 mmol) in anhydrous DMF (0.5 mL) and the mixture was stirred at rt until disappearance of the starting material (TLC monitoring, SiO₂, EtOAc/CHX/MeOH 6:3:1). Then, water (40 mL) was added affording a solid which was collected by filtration and washed with Et₂O (5 mL).

2-Amino-4-(furan-2-yl)-6-((2-hydroxyethyl)sulfanyl)pyridine-3,5-dicarbonitrile (1). Prepared from **37** according to Procedure A. TLC: SiO₂, EtOAc/CHX/MeOH 6:3:1; yield 63%; mp 171-173 °C (EtOAc/CHX). ¹H NMR (DMSO-d₆) 8.12-8.11 (m, 1H, Ar), 7.99 (br s, 2H, NH₂), 7.39 (d, *J*=3.6 Hz, 1H, Ar), 6.83 (dd, *J*=1.72, 3.6 Hz, 1H, Ar), 4.99 (t, *J*=5.4 Hz, 1H, OH), 3.65 (q, *J*=12 Hz, 2H, CH₂), 3.33 (t, *J*=6.3 Hz, 2H, CH₂); IR 3320, 3219, 2212. Anal. Calc. for C₁₃H₁₀N₄O₂S.

2-Amino-4-(furan-2-yl)-6-(2-hydroxyethoxy)pyridine-3,5-dicarbonitrile (2). Prepared from **43** according to Procedure B. Yield 56%; mp 207-209 °C (EtOH). ¹H NMR (DMSO-d₆) 8.09 (s, 1H, Ar), 8.03 (br s, 2H, NH₂), 7.38 (d, *J*=3.5 Hz, 1H, Ar), 6.84-6.83 (m, 1H, Ar), 4.91 (t, *J*=5.3 Hz, 1H, OH), 4.54-4.17 (m, 2H, OCH₂), 3.73 (dd, *J*=10.0, 5.2 Hz, 2H, CH₂). ¹³C NMR (DMSO-d₆) 166.70,

1
2
3 162.20, 146.50, 145.86, 116.47, 116.36, 115.79, 113.19, 79.48, 69.52, 64.57, 59.40 Anal. Calc. for
4
5 $C_{13}H_{10}N_4O_3$.

6
7 **2-Amino-4-(furan-2-yl)-6-((2-hydroxyethyl)amino)pyridine-3,5-dicarbonitrile (3)**. Prepared
8
9 from **32** according to Procedure C. Yield 92%; mp: 230-232 °C (EtOH). 1H NMR (DMSO- d_6) 8.03
10
11 (d, $J=0.96$ Hz, 1H, Ar), 7.33 (br s, 2H, NH_2), 7.24 (d, $J=0.56$ Hz, 1H, Ar), 7.19 (t, $J=5.4$ Hz, 1H, NH),
12
13 6.78 (dd, $J=3.5, 1.7$ Hz, 1H, Ar), 4.76 (t, $J=5.0$ Hz, 1H, OH), 3.54 (q, $J=11$ Hz, 2H, CH_2), 3.47 (q,
14
15 $J=11$ Hz, 2H, OCH_2). IR 3334, 2204. Anal. Calc. for $C_{13}H_{11}N_5O_2$.

16
17
18 **Methyl ((6-amino-3,5-dicyano-4-(furan-2-yl)pyridin-2-yl)sulfanyl)acetate (4)**.⁴³ Prepared from
19
20 **37** according to Procedure A. TLC: SiO_2 , EtOAc/CHX 1:1; yield 76%; mp 227-229 °C
21
22 (EtOAc/CHX). 1HNMR (DMSO- d_6) 8.12 (d, $J=1.12$ Hz, 1H, Ar), 8.02 (br s, 2H, NH_2), 7.42 (d, $J=3.5$
23
24 Hz, 1H, Ar), 6.84-6.85 (m, 1H, Ar), 4.19 (s, 2H, CH_2), 3.68 (s, 3H, CH_3). IR 3327, 3218, 2208. Anal.
25
26 Calc. for $C_{14}H_{10}N_4O_3S$.

27
28
29 **2-[[6-Amino-3,5-dicyano-4-(furan-2-yl)pyridin-2-yl]sulfanyl]acetamide (5)**. Prepared from **37**
30
31 according to Procedure D. Yield 73%; mp 271-273 °C dec. (EtOH/DMF). 1HNMR (DMSO- d_6) 8.11-
32
33 8.10 (m, 1H, Ar), 8.00 (br s, 2H, NH_2), 7.50 (br s, 1H, NH), 7.41 (d, $J=3.1$ Hz, 1H, Ar), 7.24 (br
34
35 s, 1H, NH), 3.87 (s, 2H, CH_2), 6.84-6.83 (m, 1H, Ar). IR 3325, 3221, 2208. Anal. Calc. for
36
37 $C_{13}H_9N_5O_2S$.

38
39
40 **2-Amino-6-((cyanomethyl)sulfanyl)-4-(furan-2-yl)pyridine-3,5-dicarbonitrile (6)**. Prepared from
41
42 **37** according to Procedure A. TLC: SiO_2 , EtOAc/CHX/MeOH 7:2:1; yield 43%; mp 297-299 °C (2-
43
44 methoxyethanol). 1H NMR (DMSO- d_6) 8.16 (br s, 2H, NH_2), 8.17-8.11 (m, 1H, Ar), 7.51-7.39 (m,
45
46 1H, Ar), 6.86 (dd, $J=3.7, 1.8$ Hz, 1H, Ar), 4.33 (s, 2H, CH_2). IR 3404, 3319, 3228, 3313, 2257, 2208.
47
48 Anal. Calc. for $C_{13}H_7N_5OS$.

49
50
51 **Benzyl 2-((6-amino-3,5-dicyano-4-(furan-2-yl)pyridin-2-yl)sulfanyl)acetate (7)**. Prepared from
52
53 **37** according to Procedure A. TLC: SiO_2 , EtOAc/CHX 1:1; yield 30%; mp 222-224 °C
54
55 (EtOAc/EtOH). 1H NMR (DMSO- d_6) 8.12 (s, 1H, Ar), 7.99 (s, 2H, NH_2), 7.42 (d, $J=3.6$ Hz, 1H, Ar),
56
57 7.41-7.20 (m, 5H, Ar), 6.85 (dd, $J=3.6, 1.7$ Hz, 1H, Ar), 5.19 (s, 2H, CH_2), 4.28 (s, 2H, SCH_2); ^{13}C
58
59
60

1
2
3 NMR (DMSO- d_6) 168.41, 166.98, 160.51, 145.44, 144.25, 136.24, 128.85, 128.54, 128.31, 116.99,
4
5 116.08, 116.01, 113.35, 89.77, 82.38, 67.10, 32.44. IR 3441, 3314, 3209, 2214, 1732. Anal. Calc. for
6
7 $C_{20}H_{14}N_4O_3S$.

8
9
10 **2-Amino-4-(furan-2-yl)-6-((2-oxo-2-phenylethyl)sulfanyl)pyridine-3,5-dicarbonitrile (8).**⁴⁴

11 Prepared from **37** according to Procedure A. TLC: SiO₂, EtOAc/CHX 1:1; yield 47%; mp 251-253
12
13 °C (EtOAc). ¹H NMR (DMSO- d_6) 8.28 (d, J=5.7 Hz, 1H, Ar), 8.08 (t, J=6.3 Hz, 2H, Ar), 7.94 (br s,
14
15 2H, NH₂), 7.93 (d, J=5.5 Hz, 1H, Ar), 7.71 (dd, J=13.4, 6.6 Hz, 1H, Ar), 7.65-7.52 (m, 2H, Ar), 6.91
16
17 (d, J=4.8 Hz, 1H, Ar), 5.01 (d, J=5.8 Hz, 2H, CH₂). IR 3485, 3350, 2206, 1618. Anal. Calc. for
18
19 $C_{19}H_{12}N_4O_2S$.

20
21
22
23 **2-Amino-4-(furan-2-yl)-6-((3-(hydroxymethyl)benzyl)sulfanyl)pyridine-3,5-dicarbonitrile (9).**

24 Prepared from **37** according to Procedure A. TLC: SiO₂, EtOAc/CHX 1:1; yield 43%; mp 193-195
25
26 °C (EtOAc). ¹H NMR (DMSO- d_6) 8.24 (s, 1H, Ar), 8.10 (br s, 2H, NH₂), 7.90 (t, J=1.6 Hz, 1H, Ar),
27
28 7.42 (s, 1H, Ar), 7.37 (d, J=7.5 Hz, 1H, Ar), 7.27 (t, J=7.5 Hz, 1H, Ar), 7.21 (d, J=7.5 Hz, 1H, Ar),
29
30 6.87 (s, 1H, Ar), 5.19 (t, J=5.7 Hz, 1H, OH), 4.55-4.43 (m, 4H, 2CH₂). IR 3398, 3314, 3215, 2214.
31
32 Anal. Calc. for $C_{19}H_{14}N_4O_2S$.

33
34
35
36
37 **Methyl 3-(((6-amino-3,5-dicyano-4-(furan-2-yl)pyridin-2-yl)sulfanyl)methyl)benzoate (10).**

38 Prepared from **37** according to Procedure A. TLC: SiO₂, EtOAc/CHX/MeOH 7:2:1; yield 62%; mp
39
40 208-210 °C (MeOH/2-methoxyethanol). ¹H NMR (DMSO- d_6) 8.09-8.08 (m, 1H, Ar), 8.00 (br s, 2H,
41
42 NH₂), 7.83-7.85 (m, 3H, Ar), 7.47 (t, J=7.72 Hz, 1H, Ar), 7.38 (d, J=3.64 Hz, 1H, Ar), 6.83 (dd,
43
44 J=1.72, 3.64 Hz, 1H, Ar), 4.58 (s, 2H, CH₂), 3.86 (s, 3H, CH₃); IR 2214, 1728. Anal. Calc. for
45
46 $C_{20}H_{14}N_4O_3S$.

47
48
49
50
51 **3-(((6-Amino-3,5-dicyano-4-(furan-2-yl)pyridin-2-yl)sulfanyl)methyl)benzamide (11).** Prepared

52 from **37** according to Procedure A. TLC: SiO₂, EtOAc/CHX/MeOH 7:2:1; yield 43%; mp: 249-251
53
54 °C (EtOH). ¹H NMR (DMSO- d_6) 8.10 (d, J=1.1 Hz, 1H, Ar), 8.07 (br s, 2H, NH₂) 7.98 (s, 1H, Ar),
55
56 7.96 (br s, 1H, NH), 7.76 (d, J=7.8 Hz, 1H, Ar), 7.68 (d, J=7.7 Hz, 1H, Ar), 7.49-7.29 (m, 3H, 2Ar +
57
58
59
60

NH), 6.83 (dd, J=3.6, 1.8 Hz, 1H, Ar), 4.53 (s, 2H, CH₂). IR 3424, 3360, 3331, 3213, 2210, 1643.

Anal. Calc. for C₁₉H₁₃N₅O₂S.

3-(((6-Amino-3,5-dicyano-4-(furan-2-yl)pyridin-2-yl)sulfanyl)methyl)benzoic acid (12).

Prepared from **37** according to Procedure A. TLC: SiO₂, EtOAc/CHX/MeOH 7:2:1; yield 35%; mp 255-257 °C (EtOH). ¹H NMR (DMSO-d₆) 13.01 (s, 1H, COOH), 8.10 (d, J=1.0 Hz, 1H, Ar), 8.05 (s, 1H, Ar), 8.13 (br s, 2H, NH₂), 7.86-7.76 (m, 2H, Ar), 7.44 (t, J=7.7 Hz, 1H, Ar), 7.39 (d, J=3.6 Hz, 1H, Ar), 6.83 (dd, J=3.6, 1.7 Hz, 1H, Ar), 4.58 (s, 2H, CH₂). IR 3329, 3327, 2214, 1541. Anal. Calc. for C₁₉H₁₂N₄O₃S.

2-Amino-6-((3-cyanobenzyl)sulfanyl)-4-(furan-2-yl)pyridine-3,5-dicarbonitrile (13). Prepared

from **37** according to Procedure A. TLC: SiO₂, EtOAc/CHX 1:1; yield 68%; mp 193-195 °C (EtOH). ¹H NMR (DMSO) 8.23 (s, 1H, Ar), 8.15 (br s, 2H, NH₂), 8.08 (s, 1H, Ar), 7.90 (dd, J=3.6, 1.8 Hz, 1H, Ar), 7.88 (d, J=8.0 Hz, 1H, Ar), 7.72 (d, J=7.7 Hz, 1H, Ar), 7.53 (t, J=7.8 Hz, 1H, Ar), 6.86 (s, 1H, Ar), 4.50 (s, 2H, CH₂). IR 3410, 3321, 3228, 2227, 2212. Anal. Calc. for C₁₉H₁₁N₅OS.

Methyl 5-(((6-amino-3,5-dicyano-4-(furan-2-yl)pyridin-2-yl)sulfanyl)methyl)furan-2-

carboxylate (14). Prepared from **37** according to Procedure A. TLC: SiO₂, EtOAc/CHX/MeOH 7:2:1; yield 64%; mp 260-262 °C (acetone). ¹H NMR (DMSO-d₆) 8.25 (s, 1H, Ar), 8.20 (br s, 2H, NH₂), 7.91 (s, 1H, Ar), 7.25 (d, J=3.5 Hz, 1H, Ar), 6.88 (s, 1H, Ar), 6.79 (d, = 3.4 Hz, 1H, Ar), 4.62 (s, 2H, CH₂), 3.80 (s, 3H, CH₃). IR 3402, 3334, 3240, 2222, 2210. Anal. Calc. for C₁₈H₁₂N₄O₄S.

2-Amino-4-(furan-2-yl)-6-((pyridin-4-ylmethyl)sulfanyl)pyridine-3,5-dicarbonitrile (15).

Prepared from **37** according to Procedure A. TLC: SiO₂, EtOAc/CHX/MeOH 7:2:1; yield 80%; mp 261-262 °C dec. (EtOH/2-metossietanolo). ¹H NMR (DMSO-d₆) 8.50 (d, J=5.9 Hz, 2H, Ar), 8.10 (d, J=1.5 Hz, 1H, Ar), 8.00 (br s, 2H, NH₂), 7.54 (d, J=5.9 Hz, 2H, Ar), 7.38 (d, J=3.6 Hz, 1H, Ar), 6.83 (dd, J=1.6 Hz, 3.6 Hz, 1H, Ar), 4.47 (s, 2H, CH₂). IR 3311, 3171, 2204, 3373, 3314, 3152, 2210, 1728. Anal. Calc. for C₁₇H₁₁N₅OS

2-Amino-4-(furan-2-yl)-6-((pyridin-3-ylmethyl)sulfanyl)pyridine-3,5-dicarbonitrile (16).

Prepared from **37** according to Procedure A. TLC: SiO₂, EtOAc/CHX/MeOH 7:2:1; yield 80%; mp

228-230 °C (MeOH). ¹H NMR (DMSO-d₆) 8.77 (d, J= 2.1 Hz, 1H, Ar), 8.45 (dd, J=4.8, 1.5 Hz, 1H, Ar), 8.89-7.52 (br s, 2H, NH₂), 8.10 (d, J=1.7 Hz, 1H, Ar), 7.94 (d, J=7.9 Hz, 1H, Ar), 7.38 (d, J=3.6 Hz, 1H, Ar), 7.34 (dd, J=7.8, 4.8 Hz, 1H, Ar), 6.83 (dd, J=3.6, 1.7 Hz, 1H, Ar), 4.49 (s, 2H, CH₂); IR 3385, 3086, 2206. Anal. Calc. for C₁₇H₁₁N₅OS

2-Amino-4-(furan-2-yl)-6-((pyridin-2-ylmethyl)sulfanyl)pyridine-3,5-dicarbonitrile (17).

Prepared from **37** according to Procedure A. TLC: SiO₂, EtOAc/CHX/MeOH 7:2:1; yield 44%; mp 212-214 °C (MeOH). ¹H NMR (DMSO-d₆) 8.48 (d, J=4.7 Hz, 1H, Ar), 8.11 (br s, 2H, NH₂), 8.00 (d, J=1.5 Hz, 1H, Ar), 7.76-7.74 (m, 1H, Ar), 7.60 (d, J=7.8 Hz, 1H, Ar), 7.37 (d, J=3.6 Hz, 1H, Ar), 7.34-7.24 (m, 1H, Ar), 6.80 (dd, J=3.6, 1.7 Hz, 1H, Ar), 4.56 (s, 2H, CH₂); ¹³C NMR (DMSO-d₆) 167.73, 160.59, 150.03, 145.54, 144.30, 137.29, 124.18, 123.00, 116.85, 116.14, 113.29, 89.68, 82.11, 35.95. IR 3389, 3311, 3148, 2206. Anal. Calc. for C₁₇H₁₁N₅OS

2-Amino-4-(furan-3-yl)-6-[(2-hydroxyethyl)sulfanyl]pyridine-3,5-dicarbonitrile (18). Prepared

from **38** according to Procedure A. TLC: SiO₂, EtOAc/CHX/MeOH 6:3:1; yield 72%; mp 191-192 °C (EtOAc/CHX). ¹H NMR (DMSO-d₆) 8.26-8.25 (m, 1H, Ar), 7.99 (br s, 2H, NH₂), 7.92 (t, J= 1.7 Hz, 1H, Ar), 6.88-6.87 (m, 1H, Ar), 4.99 (t, J=5.4 Hz, 1H, OH), 3.64 (q, J=12 Hz, 2H, CH₂), 3.33 (t, J=6.3 Hz, 2H, CH₂). Anal. Calc. for C₁₃H₁₀N₄O₂S

Methyl 3-(((6-amino-3,5-dicyano-4-(furan-3-yl)pyridin-2-yl)thio)methyl)benzoate (19).

Prepared from **38** according to Procedure A. TLC: SiO₂, EtOAc/CHX/MeOH 7:2:1; yield 61%; mp 229-231 °C (MeOH/2-methoxyethanol). ¹H NMR (DMSO-d₆) 8.24 (s, 1H, Ar), 8.09 (s, 1H, Ar), 8.34-7.77 (br s, 2H, NH₂), 7.90 (t, J=1.7 Hz, 1H, Ar), 7.85 (s, 1H, Ar), 7.83 (s, 1H, Ar), 7.47 (t, J=7.7 Hz, 1H, Ar), 6.87 (d, J=1.8 Hz, 1H, Ar), 4.58 (s, 2H, CH₂), 3.86 (s, 3H, CH₃). IR 3373, 3113, 2210, 1527. Anal. Calc. for C₂₀H₁₄N₄O₃S

2-Amino-6-((2-hydroxyethyl)sulfanyl)-4-(thiophen-2-yl)pyridine-3,5-dicarbonitrile (20).⁴⁵

Prepared from **39** according to Procedure A. TLC: SiO₂, EtOAc/CHX/MeOH 6:3:1; yield 76%; mp 154-156 °C (AcOEt/CHX). ¹H NMR (DMSO-d₆) 8.03 (br s, 2H, NH₂), 7.94 (d, J=4.9 Hz, 1H, Ar),

7.55 (d, J=3.4 Hz, 1H, Ar), 7.28 (d, J=4 Hz, 1H, Ar), 4.99 (t, J=5.4 Hz, 1H, OH), 3.65 (q, J=12 Hz, 2H, CH₂), 3.33 (t, J=6.3 Hz, 2H, CH₂). IR 3320, 3222, 2208. Anal. Calc. for C₁₃H₁₀N₄OS₂.

2-Amino-6-((2-hydroxyethyl)amino)-4-(thiophen-2-yl)pyridine-3,5-dicarbonitrile (21).⁴⁵

Prepared from **34** according to Procedure C. Yield 88%; 220-222 °C (EtOH). ¹H NMR (DMSO-d₆) 7.87 (d, J=4.7 Hz, 1H, Ar), 7.47 (d, J=1.6 Hz, 1H, Ar), 7.42 (br s, 2H, NH₂), 7.26-7.22 (m, 2H, NH + Ar), 4.74 (t, J=5.1 Hz, 1H, OH), 3.54 (q, J=10.9 Hz, 2H, CH₂), 3.48 (q, J=10.9, 2H, OCH₂). IR 3491, 3451, 3338, 2202. Anal. Calc. for C₁₃H₁₁N₅OS.

Methyl 3-(((6-amino-3,5-dicyano-4-(thiophen-2-yl)pyridin-2-yl)sulfanyl)methyl)benzoate (22).

Prepared from **39** according to Procedure A. TLC: SiO₂, EtOAc/CHX/MeOH 7:2:1; yield 76%; mp 199-201 °C (EtOH). ¹H NMR (DMSO-d₆) 8.10 (s, 1H, Ar), 7.94 (d, J=5.0 Hz, 1H, Ar), 8.55-7.72 (m, 2H, NH₂), 7.86 (s, 1H, Ar), 7.84 (s, 1H, Ar), 7.56 (d, J=2.7 Hz, 1H, Ar), 7.47 (t, J=7.7 Hz, 1H, Ar), 7.27 (dd, J=4.9, 3.8 Hz, 1H, Ar), 4.59 (s, 2H, CH₂), 3.86 (s, 3H, CH₃). IR 3462, 3329, 3217, 2210, 1547. Anal. Calc. for C₂₀H₁₄N₄O₂S₂

2-Amino-6-((2-hydroxyethyl)sulfanyl)-4-(thiophen-3-yl)pyridine-3,5-dicarbonitrile (23).

Prepared from **40** according to Procedure A. TLC: SiO₂, EtOAc/CHX/MeOH 6:3:1; yield 60%; mp 175-178 °C (EtOAc/CHX). ¹H NMR (DMSO-d₆) 8.03 (q, 1H, J=2.9 Hz, Ar), 7.95 (br s, 2H, NH₂), 7.76 (q, J=5.0 Hz, 1H, Ar), 7.38 (dd, J=1.3 Hz, 5.0 Hz, 1H, Ar), 5.00 (br s, 1H, OH), 3.65 (t, J=6.4 Hz, 2H, CH₂), 3.34 (t, J=6.4 Hz, 2H, CH₂). IR 3320, 3209, 2212. Anal. Calc. for C₁₃H₁₀N₄OS₂.

2'-Amino-6'-((2-hydroxyethyl)sulfanyl)-3,4'-bipyridine-3',5'-dicarbonitrile (24). Prepared from

41 according to Procedure A. TLC: SiO₂, EtOAc/CHX/MeOH 6:3:1; yield 98%; mp 233-235 °C (EtOAc/CHX). ¹H NMR (DMSO-d₆) 8.81-8.51 (m, 1H, Ar), 8.10 (br s, 2H, NH₂), 8.04-8.01 (m, 2H, ar), 7.63-7.52 (m, 1H, Ar), 5.01 (t, J=5.2 Hz, 1H, OH), 3.67 (q, J= 11.5 Hz, 2H, CH₂), 3.36 (t, J=6.3 Hz, 2H, CH₂). IR 3319, 3124, 2212. Anal. Calc. for C₁₄H₁₁N₅OS.

2-Amino-6-((2-hydroxyethyl)amino)-4-(pyridin-3-yl)pyridine-3,5-dicarbonitrile (25). Prepared

from **36** according to Procedure C. Yield 79%; mp 251-253 °C (EtOH). ¹H NMR (DMSO-d₆): 8.74 (d, J=4.1, Hz 1H, Ar), 8.69 (s, 1H, Ar), 7.96 (d, J=7.9 Hz, 1H, Ar), 7.61-7.58 (m, 1H, Ar), 7.60-7.40

(br s, 2H, NH₂), 7.33 (t, J=5.2 Hz, 1H, NH), 4.74 (t, J=5.1 Hz, 1H, OH), 3.57-3.54 (m, 2H, CH₂), 3.51-3.48 (m, 2H, CH₂). IR 3306, 2206, 1633, 1099, 1026. Anal. Calc. for C₁₄H₁₂N₆O

Methyl 3-(((6'-amino-3',5'-dicyano-(3,4'-bipyridin)-2'-yl)thio)methyl)benzoate (26). Prepared from **41** according to Procedure A. TLC: SiO₂, EtOAc/CHX/MeOH 7:2:1; yield 21%; mp 222-224 °C (2-methoxyethanol/EtOH); ¹H NMR (DMSO-d₆) 8.83-8.67 (m, 2H, Ar), 8.23 (br s, 2H, NH₂), 8.11 (s, 1H, Ar), 8.03 (d, J=7.9 Hz, 1H, Ar), 7.86 (t, J = 7.8 Hz, 2H, Ar), 7.61 (dd, J=7.7, 4.9 Hz, 1H, Ar), 7.48 (t, J=7.7 Hz, 1H, Ar), 4.61 (s, 2H, CH₂), 3.86 (s, 3H, CH₃); ¹³C NMR (100 MHz, DMSO-d₆): 166.44, 159.88, 155.82, 151.73, 149.01, 139.08, 136.86, 134.89, 130.65, 130.36, 129.29, 128.51, 124.01, 115.48, 93.84, 86.77, 52.65, 33.05. Anal. Calc. for C₂₁H₁₅N₅O₂S

2-(Cyclopentylamino)-4-(furan-2-yl)-6-((2-hydroxyethyl)sulfanyl)pyridine-3,5-dicarbonitrile (27). Prepared from **44** according to Procedure E. Yield: 89%; mp 185-187 °C (MeOH). ¹H NMR (DMSO-d₆) 8.10 (s, 1H, Ar), 7.83 (d, J=6.8 Hz, 1H, NH), 7.36 (d, J=3.5 Hz, 1H, Ar), 6.82 (s, 1H, Ar), 5.03 (t, J=5.3 Hz, 1H, OH), 4.60-4.37 (m, 1H, CH), 3.67 (dd, J=12.1, 6.2 Hz, 2H, OCH₂), 3.31 (t, J=6.2 Hz, 2H, SCH₂) 1.96 (dd, J=10.6, 6.4 Hz, 2H, CH₂), 1.82-1.46 (m, 6H, 3CH₂); ¹³C NMR (DMSO-d₆) 168.59, 157.83, 145.56, 144.17, 116.73, 116.31, 116.07, 113.23, 89.74, 83.21, 59.98, 53.70, 33.33, 32.26, 24.29. IR 3466, 3348, 2210. Anal. Calc. for C₁₈H₁₈N₄O₂S

2-(Cyclopropylamino)-4-(furan-2-yl)-6-((2-hydroxyethyl)sulfanyl)pyridine-3,5-dicarbonitrile (28). Prepared from **44** according to Procedure E. Yield 91%; mp 214-216 °C (MeOH). ¹H NMR (DMSO-d₆) 8.29 (br s, 1H, NH), 8.10 (s, 1H, Ar), 7.37 (d, J=3.4 Hz, 1H, Ar), 6.84 (s, 1H, Ar), 5.01 (t, J=5.4 Hz, 1H, OH), 3.70 (dd, J=12.1, 6.2 Hz, 2H, OCH₂), 3.38 (t, J=6.5 Hz, 2H, CH₂), 2.97-2.84 (m, 1H, CH), 0.80 (m, 2H, CH eq), 0.75-0.61 (m, 2H, CH ax). IR 3491, 3302, 2210. Anal. Calc. for C₁₆H₁₄N₄O₂S

4-(Furan-2-yl)-2-((2-hydroxyethyl)thiosulfanyl)-6-((4-iodophenyl)amino)pyridine-3,5-dicarbonitrile (29). Prepared from **44** according to Procedure E. Yield 99%; mp 218-220 °C (acetone). ¹H NMR (DMSO-d₆) 9.93 (br s, 1H, NH), 8.15 (s, 1H, Ar), 7.72 (d, J=8.5 Hz, 2H, Ar), 7.45 (d, J=3.5 Hz, 1H, Ar), 7.38 (d, J=8.6 Hz, 2H, Ar), 6.96-6.78 (m, 1H, Ar), 4.96 (t, J=5.8 Hz, 1H,

OH), 3.58-3.46 (m, 2H, OCH₂), 3.16 (t, J=6.1 Hz, 2H, SCH₂); ¹³C NMR (DMSO-d₆) 178.96, 168.75, 156.80, 145.36, 144.60, 138.22, 137.53, 126.43, 117.20, 115.92, 115.83, 113.36, 92.69, 89.73, 59.82, 33.60. IR 3394, 3296, 2216. Anal. Calc. for C₁₉H₁₃IN₄O₂S

2-(Benzylamino)-4-(furan-2-yl)-6-((2-hydroxyethyl)sulfanyl)pyridine-3,5-dicarbonitrile (30).

Prepared from **44** according to Procedure E. Yield 86%; mp: 171-173 °C (MeOH). ¹H NMR (DMSO-d₆) 8.80 (s, 1H, NH), 8.11 (s, 1H, Ar), 7.40 (d, J=3.5 Hz, 1H, Ar), 7.38-7.29 (m, 4H, Ar), 7.25 (s, 1H, Ar), 6.85 (s, 1H, Ar), 4.98 (t, J=5.4 Hz, 1H, OH), 4.70 (d, J=5.4 Hz, 2H, CH₂), 3.48 (dd, J=11.6, 5.9 Hz, 2H, OCH₂), 3.16 (t, J=6.1 Hz, 2H, SCH₂); ¹³C NMR (DMSO-d₆): 168.81, 158.22, 145.51, 144.02, 139.43, 128.80, 127.35, 116.83, 116.22, 116.08, 113.29, 90.03, 83.13, 59.74, 45.18, 33.42. IR 3344, 2208. Anal. Calc. for C₂₀H₁₆N₄O₂S.

Synthesis of N-(3,5-dicyano-4-(furan-2-yl)-6-((2-hydroxyethyl)thio)pyridin-2-yl)acetamide (31).

Sodium hydrogen carbonate (0.53 mmol) and 2-bromoethanol (0.39 mmol) were sequentially added to a stirred solution of compound **46**⁵⁴ (0.35 mmol) in anhydrous DMF (1 mL). The reaction mixture was kept at rt for 3h and then water (10 mL) was added affording a light brown solid which was filtered and washed with water (10 mL) and Et₂O (5 mL). The crude product was purified by preparative TLC on silica gel using EtOAc as eluting system, and then recrystallized. Yield 20%; mp 164-166 °C (MeOH). ¹H NMR (DMSO-d₆) 11.13 (s, 1H, NH), 8.21 (s, 1H, Ar), 7.53 (d, J=3.6 Hz, 1H, Ar), 6.90 (dd, J=3.6, 1.7 Hz, 1H, Ar), 5.07 (s, 1H, OH), 3.70 (t, J=6.2 Hz, 2H, OCH₂), 3.42 (t, J=6.2 Hz, 2H, SCH₂), 2.21 (s, 3H, CH₃); ¹³C NMR (DMSO-d₆) 169.37, 168.55, 155.12, 144.96, 144.30, 118.22, 115.22, 115.09, 113.76, 113.27, 98.59, 94.79, 59.69, 33.87, 24.06; IR 3321, 2218, 1718. Anal. Calc. for C₁₅H₁₂N₄O₃S.

Synthesis of 2-amino-4-(furan-3-yl)-6-(phenylsulfanyl)pyridine-3,5-dicarbonitrile (33).

A solution of 3-furaldehyde (10 mmol), malononitrile (20 mmol) and tetrabutylammonium fluoride hydrate (10% mol) in water (50 mL), was stirred at rt for 20 min. Then, thiophenol (10 mmol) was

1
2
3 added and the mixture was heated at 80 °C for 2 h. After cooling at rt, the water was removed under
4
5 reduced pressure, the residue dissolved in EtOAc (100 mL) and the resulting solution dried over
6
7 anhydrous sodium sulfate. After distillation of the solvent, the crude product was triturated with a
8
9 mixture of Et₂O/EtOH (10:1), collected by filtration and recrystallized. Yield 22%; mp 204-206 °C
10
11 (MeOH). ¹H NMR (DMSO-d₆) 8.29-8.22 (m, 1H, Ar), 7.94-7.93 (m, 1H, Ar), 7.81 (br s, 2H, NH₂),
12
13 7.60-7.59 (m, 2H, Ar), 7.51-7.50 (m, 3H, Ar), 6.91-6.90 (m, 1H, Ar). IR 3328, 3218, 2220. Anal.
14
15 Calc. for C₁₇H₁₀N₄OS

16
17
18
19
20
21 **Synthesis of 2-amino-4-(furan-3-yl)-6-sulfanylpuridine-3,5-dicarbonitrile (38).** To a stirred
22
23 solution of compound **33** (10 mmol) in anhydrous DMF (1 mL) maintained at rt and under nitrogen
24
25 atmosphere, an excess of anhydrous sodium sulfide (33 mmol) was added. The reaction mixture was
26
27 heated at 80 °C for 2 h. Then, 1N HCl (25 mL), followed by 6N HCl, was drop by drop added to
28
29 obtain a precipitate which was collected by filtration, washed with water (20 ml) and Et₂O (5 ml),
30
31 and recrystallized. Yield 92%; mp 260-262 °C (EtOH). ¹H NMR (DMSO-d₆) 12.97 (br s, 1H, SH),
32
33 8.27-8.25 (m, 1H, Ar), 8.00 (br s, 2H, NH₂), 7.90 (t, J=1.6 Hz, 1H, Ar), 6.85- 6.84 (m, 1H, Ar); IR
34
35 3307, 3192, 2216. Anal. Calc. for C₁₁H₆N₄OS

36
37
38
39
40
41
42 **Synthesis of 2-amino-4-(furan-2-yl)-6-methoxypyridine-3,5-dicarbonitrile (42).**⁵² A solution of
43
44 sodium methoxide (30.4 mmol) in MeOH (20 mL) was rapidly added to a solution of 2-furaldehyde
45
46 (20.8 mmol), malononitrile (20.8 mmol) and tetrabutylammonium fluoride hydrate (2.1 mmol) in
47
48 MeOH (10 mL) at rt. Then, a further amount of malononitrile (20.8 mmol) was added and the mixture
49
50 was refluxed for 3h. The resulting suspension was filtered over celite pad and the filtrate evaporated
51
52 under reduced pressure. The crude residue was purified by silica gel column chromatography, CH₂Cl₂
53
54 as eluting system. Yield 27%; mp 205-207 °C (EtOH). ¹H NMR (DMSO-d₆) 8.09 (s, 1H, Ar), 8.05
55
56 (br s, 2H, NH₂), 7.38 (s, 1H, Ar), 6.83 (s, 1H, Ar), 3.97 (s, 3H, CH₃); IR 3406, 3345, 3244, 2222.
57
58
59 Anal. Calc. for C₁₂H₈N₄O₂

Synthesis of 2-amino-4-(furan-2-yl)-6-hydroxypyridine-3,5-dicarbonitrile (43)⁵³

Compound **42**⁵² (1.4 mmol) was suspended in a mixture of glacial acetic acid (4 mL) and concentrated HCl (1 mL), and heated at 100 °C for 2 h. Then, the reaction mixture was cooled at rt affording a precipitate which was collected by filtration, washed with water (20 mL) and Et₂O (5 mL) and dried in oven at 60 °C. Yield 81%; mp 186-188 °C (EtOH). ¹H NMR (DMSO-d₆) 11.85 (br s, 1H, OH), 8.08 (d, J=1.1 Hz, 1H, Ar), 7.72 (br s, 2H, NH₂), 7.36 (d, J=3.6 Hz, 1H, Ar), 6.82 (dd, J=3.6, 1.7 Hz, 1H, Ar); IR 3319, 3199, 2226, 2212. Anal. Calc. for C₁₁H₆N₄O₂

Synthesis of 2-chloro-4-(furan-2-yl)-6-((2-hydroxyethyl)thio)pyridine-3,5-dicarbonitrile (44).

Isoamylnitrite (9 mmol) was added to a suspension of copper (II) chloride (9 mmol) in anhydrous CH₃CN (5 mL) under nitrogen atmosphere. The reaction mixture was stirred 20 min at rt. Then, compound **1** (1.5 mmol) was added and the reaction was maintained at rt for a weekend. 1N HCl was added until pH 1 and the resulting mixture was extracted with CH₂Cl₂ (4 x 25 mL). The collected organic layers were washed with brine (2 x 20 mL) and dried (Na₂SO₄). The solvent was removed under reduced pressure and the yellow residue triturated with Et₂O (2 mL), filtered and recrystallized. Yield 67 %; mp 197-199 °C (EtOH). ¹H NMR (DMSO-d₆) 8.27 (s, 1H,Ar), 7.66 (d, J=3.6 Hz, 1H, Ar), 6.95 (d, J=3.6 Hz, 1H, Ar), 3.70 (t, J=6.3 Hz, 2H, CH₂), 3.41(t, J=6.3 Hz, 2H, CH₂); IR 2230. Anal. Calc. for C₁₃H₈ClN₃O₂S

Synthesis of N-(3,5-dicyano-4-(furan-2-yl)-6-(phenylsulfanyl)pyridin-2-yl)acetamide (45).

A solution of compound **32**⁴⁶ (0.94 mmol) and anhydrous pyridine (0.23 mmol) in acetic anhydride (2 mL) was refluxed for 28h. After removal of the solvent under reduced pressure, a brown solid was obtained which was purified by silica gel column chromatography, eluting system CHX /EtOAc 7:3.

1
2
3 Yield 41%; mp 213-215 °C (EtOH). ¹H NMR (DMSO-d₆) 10.82 (s, 1H, NH), 8.23 (d, J=1.2 Hz, 1H,
4 Ar), 7.69-7.62 (m, 2H, Ar), 7.54 (m, J=15.1, 4.6 Hz, 4H, Ar), 6.92 (dd, J=3.7, 1.8 Hz, 1H, Ar), 1.92
5
6 (s, 3H, CH₃); IR 3358, 3147, 2216, 1705. Anal. Calc. for C₁₉H₁₂N₄O₂S
7
8
9

10
11
12 **Synthesis of N-(3,5-dicyano-4-(furan-2-yl)-6-sulfanylpyridin-2-yl)acetamide (46).**⁵⁴ Sodium
13 sulfide (1.2 mmol) was added to a solution of compound **45** (0.36 mmol) in anhydrous DMF (0.5
14 mL), and the reaction mixture was heated at 80 °C for 3h. Then, 0.1N HCl (25 mL) was added
15 followed by addition of 6N HCl until an abundant precipitate formed. The solid was collected by
16 filtration, washed with water (20 mL) and Et₂O (5 mL), and used for the next step without any further
17 purification. Yield 98%. ¹H NMR (DMSO-d₆) 12.99 (s, 1H, SH), 11.25 (br s, 1H, NH), 8.19 (s, 1H,
18 Ar), 7.50 (d, J=3.4 Hz, 1H, Ar), 6.89 (s, 1H, Ar), 2.23 (s, 3H, CH₃). Anal. Calc. for C₁₃H₈N₄O₂S
19
20
21
22
23
24
25
26
27
28
29

30 **Pharmacological assays**

31
32
33 **Cell culture and membrane preparation.** Wild type CHO cells and hA₁, hA_{2A}, hA_{2B} and hA₃ ARs
34 CHO cells were cultured in Dulbecco's modified Eagle's medium with nutrient mixture F12,
35 containing 10% fetal calf serum, penicillin (100 U/ml), streptomycin (100 µg/ml), l-glutamine (2
36 mM), geneticine (G418; 0.2 mg/ml) at 37°C in 5% CO₂/95% air⁷⁶. To obtain membranes, the cells
37 were washed with phosphate-buffered saline and resuspended in ice-cold hypotonic buffer (5 mM
38 Tris HCl, 1 mM EDTA, pH 7.4). The cells were homogenized by using a Polytron, centrifuged for
39 30 min at 40000 g at 4°C and the resulting membranes were used in binding experiments⁷⁶.
40
41
42
43
44
45
46
47
48

49 **Saturation binding assays.** [³H]DPCPX (0.01 to 10 nM), [³H]ZM241385 (0.01 to 10 nM) and
50 [¹²⁵I]AB-MECA (0.01 to 10 nM) were used in the saturation binding experiments as radioligands for
51 hA₁, hA_{2A} and hA₃ ARs, respectively. The radioligands and membranes (50 mg of protein per assay)
52 were incubated at 25°C, 90 min for hA₁ARs, at 4°C, 60 min for hA_{2A}ARs and at 4°C, 120 min for
53 hA₃ARs.
54
55
56
57
58
59
60

1
2
3 **Competition binding assays.** The affinity to hA₁, hA_{2A} and hA₃ ARs of the novel compounds was
4 studied. Human A₁ ARs competition experiments were performed incubating [³H]-8-cyclopentyl-1,3-
5 dipropylxanthine at 1 nM concentration ([³H]-DPCPX, K_D = 1.12 ± 0.11 nM) with 50 µg of
6 protein/100 µl membranes and various concentrations of the newly synthesized compounds in 50 mM
7 Tris HCl, pH 7.4 at 25°C for 90 min. Non-specific binding was calculated in the presence of 1 µM
8 DPCPX and was minor than 10% of the total binding⁷⁶. Human A_{2A} ARs inhibition binding assays
9 were carried out incubating 1 nM of [³H]-ZM241385 (K_D = 1.25 ± 0.13 nM) with membranes (50 µg
10 of protein/100 µl) and the examined compounds at different concentrations at 4°C for 60 min in 50
11 mM Tris HCl (pH 7.4) with 10 mM of MgCl₂. The presence of 1 µM ZM241385 was used as a
12 condition to evaluate non-specific binding that was about 20% of the total binding⁷⁷. Human A₃ ARs
13 competition binding experiments were executed incubating 50 µg of protein/100 µl of membranes
14 with 0.5 nM [¹²⁵I]-N⁶-(4-aminobenzyl)-N-methylcarboxamidoadenosine ([¹²⁵I]-ABMECA, K_D = 0.85
15 ± 0.07 nM) in the presence of the novel compounds for 120 min at 4°C in 50 mM Tris HCl buffer
16 (pH 7.4), 10 mM MgCl₂, 1 mM EDTA. The presence of 1 µM ABMECA was utilized to evaluate
17 non-specific binding that was minor than 10% of the total binding⁷⁸. Each in vitro assay includes four
18 independent experiments, each performed in triplicate.

19
20
21
22
23
24
25
26
27
28
29
30
31
32
33
34
35
36
37
38
39
40
41
42
43
44
45
46
47
48
49
50
51
52
53
54
55
56
57
58
59
60
The samples were filtered in a Brandel cell harvester (Brandel Instruments, Unterföhring, Germany)
to separate bound and free radioactivity by using Whatman GF/B glass fiber filters. Bound
radioactivity was counted by means of a Packard Tri Carb 2810 TR scintillation counter (Perkin
Elmer).

Cyclic AMP assays. Wild type CHO cells and CHO cells transfected with hA₁, hA_{2A} and hA_{2B} ARs
were washed with phosphate-buffered saline, trypsinized and centrifuged at 200 g for 10 min. Cells
were plated in 96-well white half-area microplate (Perkin Elmer, Boston, USA) in a buffer Hank
Balanced Salt Solution containing 5 mM HEPES, 0.5 mM Ro 20-1724, 0.1% BSA, 1 IU/ml adenosine
deaminase. The novel compounds at the final concentrations from 1 nM to 1 µM were tested alone
and/or in the presence of CCPA 1 nM (for hA₁AR), CGS 21680 10 nM (for hA_{2A}AR) or NECA 100

1
2
3 nM (for hA_{2B}AR). AlphaScreen cAMP Detection Kit (Perkin Elmer, Boston, USA) was used to
4
5 quantified cAMP levels following the manufacturer's instructions⁷⁹. Perkin Elmer EnSight
6
7 Multimode Plate Reader was used to read the plates. Each in vitro assay includes four independent
8
9 experiments, each performed in triplicate.

10
11
12 **Data Analysis.** A Bio-Rad method with bovine albumin as a standard reference was used to the
13
14 evaluation of the protein concentration. From the IC₅₀ values obtained in competition binding
15
16 experiments, inhibitory binding constant (K_i) values were evaluated using the Cheng & Prusoff
17
18 equation $K_i = IC_{50}/(1+[C^*]/K_D^*)$, where [C*] is the radioligand concentration and K_D* its dissociation
19
20 constant.⁷⁸ Affinity (K_i) and potency (IC₅₀) values were obtained by non-linear regression analysis
21
22 using the equation for a sigmoid concentration-response curve (Graph-PAD Prism, San Diego, CA,
23
24 U.S.A).

25
26
27
28 **Animals.** Male CD-1 albino mice (Envigo, Varese, Italy) weighing approximately 22–25 g (three
29
30 months of age) at the beginning of the experimental procedure, were used. Animals were housed in
31
32 CeSAL (Centro Stabulazione Animali da Laboratorio, University of Florence) and used at least 1
33
34 week after their arrival. Ten mice were housed per cage (size 26 × 41 cm); animals were fed a standard
35
36 laboratory diet and tap water *ad libitum*, and kept at 23 ± 1 °C with a 12 h light/dark cycle, light at 7
37
38 a.m. All animal manipulations were carried out according to the Directive 2010/63/EU of the
39
40 European parliament and of the European Union council (22 September 2010) on the protection of
41
42 animals used for scientific purposes. The ethical policy of the University of Florence complies with
43
44 the Guide for the Care and Use of Laboratory Animals of the US National Institutes of Health (NIH
45
46 Publication No. 85-23, revised 1996; University of Florence assurance number: A5278-01). Formal
47
48 approval to conduct the experiments described was obtained from the Animal Subjects Review Board
49
50 of the University of Florence. Experiments involving animals have been reported according to
51
52 ARRIVE guidelines.⁸⁰ All efforts were made to minimize animal suffering and to reduce the number
53
54 of animals used.
55
56
57
58
59
60

1
2
3 **Oxaliplatin-induced neuropathic pain model.** Mice treated with oxaliplatin (2.4 mg kg⁻¹) were
4 administered i.p. on days 1-2, 5-9, 12-14 (10 i.p. injections) .⁸¹ Oxaliplatin was dissolved in 5%
5 glucose solution. Control animals received an equivalent volume of vehicle. Behavioral tests were
6 performed on day 15.
7
8
9

10
11 **Cold Plate Test.** The animals were placed in a stainless steel box (12 cm × 20 cm × 10 cm) with a
12 cold plate as floor. The temperature of the cold plate was kept constant at 4°C ± 1°C. Pain-related
13 behavior (licking of the hind paw) was observed and the time (seconds) of the first sign was recorded.
14
15
16
17
18
19 The cut-off time of the latency of paw lifting or licking was set at 60 seconds.⁸²
20

21 **Compound administrations.** Compound 9-12 were dissolved in 1% CMC and orally administered.
22
23 Measurements were performed 15, 30, 45, 60 and 75 min after injection. Control mice were treated
24 with vehicle. The non-selective nAChR antagonist mecamylamine (meca; 2 mg kg⁻¹ i.p.) and the
25 selective alpha7 nAChR antagonist methyllycaconitine (MLA; 6 mg kg⁻¹ i.p.) were administered 15
26 min before tested compounds. Measurements were performed 15, 30, 45, and 60 min after the
27 injection of tested compounds. Control mice were treated with vehicle.
28
29
30
31
32
33

34
35 **Statistical analysis.** Behavioural measurements were performed on 10 mice for each treatment
36 carried out in 2 different experimental sets. Results were expressed as mean ± S.E.M. The analysis
37 of variance of behavioural data was performed by one way ANOVA, a Bonferroni's significant
38 difference procedure was used as post-hoc comparison. *P* values of less than 0.05 or 0.01 were
39 considered significant. Investigators were blind to all experimental procedures. Data were analyzed
40 using the “Origin 9” software (OriginLab, Northampton, USA).
41
42
43
44
45
46
47
48
49

50 **Molecular modelling**

51
52 Receptor refinement and energy minimization tasks were carried out using Molecular Operating
53 Environment (MOE, version 2014.09) suite.⁵⁷ Docking experiments were performed with CCDC
54 Gold⁵⁸ and Autodock (within PyRx interface) .⁵⁹⁻⁶¹ All ligand structures were optimized using
55
56
57
58
59
60

1
2
3 RHF/AM1 semi-empirical calculations and the software package MOPAC⁸³ implemented in MOE
4
5 was utilized for these calculations.
6

7 **A₁AR and A_{2A}AR crystal structures refinement.** The recently published crystal structure of the
8
9 human A₁AR and the crystal structure of the human A_{2A}AR in complex with the covalently bound
10
11 ligand DU172 and inverse agonist ZM241385, respectively, were downloaded by the Protein Data
12
13 Bank webpage (<http://www.rcsb.org>; pdb code: 5UEN; 3.2-Å resolution⁵⁶ and pdb code: 4E1Y; 1.8-
14
15 Å resolution,⁶² respectively). The A₁AR was then rebuilt by removing the covalently bound ligand
16
17 DU172 and the engineered segment bRIL and by restoring the IL3 missing loop and the wild type
18
19 receptor sequence that was changed with the Asn159Ala mutation inserted in the X-ray structure. The
20
21 Homology Modeling tool of MOE was used for these tasks. The A_{2A}AR crystal structure was used in
22
23 its original form to which all hydrogen atoms were added within MOE. The protein structures were
24
25 then energetically minimized with MOE using the AMBER99 force field until the RMS gradient of
26
27 the potential energy was less than 0.05 kJ mol⁻¹ Å⁻¹. Reliability and quality of the models were
28
29 checked using the Protein Geometry Monitor application within MOE, which provides a variety of
30
31 stereo-chemical measurements for inspection of the structural quality in a given protein, like
32
33 backbone bond lengths, angles and dihedrals, Ramachandran φ-ψ dihedral plots, and sidechain-
34
35 rotamer and non-bonded contact quality.
36
37
38
39
40

41
42 **Homology modeling of the human A₃AR structure.** A homology model of the human A₃AR was
43
44 built using the above cited X-ray structure of the antagonist-bound A₁AR as templates (pdb code:
45
46 5UEN)³⁴. A multiple alignment of the AR primary sequences was built within MOE as preliminary
47
48 step. The Homology Modelling tool of MOE was employed even for this task. The obtained A₃AR
49
50 model was then energetically minimized with the same protocol of the other receptors (see above).
51
52

53 **Molecular docking analysis.** Docking analyses were performed by using CCDC Gold⁵⁸ and
54
55 Autodock.^{59,60} Gold tool was used with default efficiency settings through MOE interface, by
56
57 selecting ChemScore as scoring function and 50 poses to be generated for each ligand. Autodock
58
59 4.2.6 software was used with PyRx⁶¹ interface. Lamarckian genetic algorithm was employed for this
60

analysis with the following settings: 50 runs for each ligand; 2,500,000 as maximum number of energy evaluations; 27,000 as maximum number of generations; 0.02 as rate of gene mutation and 0.8 as rate of crossover. The grid box was set with 50, 50, and 50 points in the x , y , and z directions, respectively, with the default grid spacing of 0.375 Å.

Post Docking analysis. Residue interaction analysis. The interactions between the ligands and the A₁AR receptors binding site were analyzed by using the *IF-E 6.0* tool retrievable at the SVL exchange service (Chemical Computing Group, Inc. SVL exchange: <http://svl.chemcomp.com>). The program calculates and displays the atomic and residue interaction forces as 3D vectors. It also calculates the per-residue interaction energies, where negative and positive energy values are associated to favorable and unfavorable interactions, respectively. For each A₁AR structure, a shell of residues contained within a 10 Å distance from ligand were considered for this analysis.

Stability studies

Chemicals. Acetonitrile, ethanol (Chromasolv), formic acid and (MS grade), NaCl, KCl, Na₂HPO₄ 2H₂O, KH₂PO₄ (Reagent grade), 2-[[6-Amino-3,5-dicyano-4-(4-(cyclopropylmethoxy)phenyl)pyridin-2-yl]thio]acetamide (BAY60-6583, used as internal standard), Enalapril and Ketoprofen (analytical standard) were purchased by Sigma-Aldrich (Milan, Italy). Ketoprofen Ethyl Ester (KEE) were obtained by Fisher's reaction from Ketoprofen and ethanol. MilliQ water 18 MΩ was obtained from Millipore's Simplicity system (Milan - Italy). Phosphate buffer solution (PBS) was prepared by adding 8.01 g L⁻¹ of NaCl, 0.2 g L⁻¹ of KCl, 1.78 g L⁻¹ of Na₂HPO₄ * 2H₂O and 0.27 g L⁻¹ of KH₂PO₄. Human plasma was collected from healthy volunteer and was kept at -80 °C until use. Sprague Dawley male rat plasma was heparinized, filtered and kept at -80 °C until use.

Instrumental. The LC-MS/MS analysis was carried out using a Varian 1200L triple quadrupole system (Palo Alto, CA, USA) equipped by two Prostar 210 pumps, a Prostar 410 autosampler and an Elettrospray Source (ESI) operating in negative ions. The ion sources and ion optics parameters were

1
2
3 optimized during the calibration of the instrument introducing, via syringe pump at $10 \mu\text{L min}^{-1}$, a 1
4
5 $\mu\text{g mL}^{-1}$ tuning solution.
6

7 Raw-data were collected and processed by Varian Workstation Vers. 6.8 software.
8

9
10 G-Therm 015 thermostatic oven was used to maintained the samples at $37 \text{ }^\circ\text{C}$ during the stability test.
11

12 **Method LC-MS/MS.** The chromatographic parameters employed to analyse the samples were tuned
13
14 to minimize the run time and were reported as follows:
15

16
17 - column, Pursuit XRs C18 length = 30 mm internal diameter= 2mm; particle size = $3 \mu\text{m}$ purchased
18
19 from Agilent Technologies (Palo Alto, CA, USA)
20

21 - acidic mobile phase, composed by 10mM of formic acid solution (solvent A) and 10 mM of formic
22
23 acid in acetonitrile (solvent B).
24

25
26 - flow rate and the injection volume were 0.25 mL min^{-1} and $5 \mu\text{L}$ respectively.
27

28 The elution gradient is shown in Table 6.
29

30 The analyses were acquired in Multiple Reaction Monitoring (MRM), parameters are reported in
31
32 Table 7, using 100 ms of dwell time and argon at 2.0 mTorr as collision gas.
33
34
35
36

37 **Table 6.** Elution gradient of mobile phase used for LC-MS/MS analyses.
38

Time (min)	A (%)
0.00	90
4.00	10
6.00	10
6.01	90
8.00	90

Table 7. MRM parameters.

Compd	Precursor Ion (m/z)	Quantifier Ion (m/z) [collision energy (V)]	Qualifier Ion (m/z) [collision energy (V)]
10	389	209 [25]	362 [15]
BAY60-6583	378	304 [20]	249 [30]
KEE	283	209 [10]	105 [25]
Enalapril	377	234 [15]	303 [15]

Standard solutions and calibration curves. Stock solutions of analyte and internal standard (ISTD) were prepared in acetonitrile at 1.0 mg mL⁻¹ and stored at 4 °C. Working solutions of analyte were freshly prepared by diluting stock solution up to a concentration of 10 µM and 1 µM (Working solution 1 and 2 respectively) in mixture of mQ water/acetonitrile 80:20 (v/v). The ISTD working solution was prepared in acetonitrile at 25 ng mL⁻¹ (ISTD solution).

A six levels calibration curve was prepared by adding proper volumes of working solution 1 or 2 to a constant volume of ISTD solution (300 µL corresponding to 7.5 ng of ISTD). The obtained solutions were dried under a gentle nitrogen stream and dissolved in 1.5 mL of mQ water/acetonitrile 80:20 (v/v) added with 10 mM of formic acid. Final concentrations of calibration levels were: 0; 0.10; 0.20; 0.50; 0.75 and 1.00 µM.

All calibration levels were analyzed six times by LC-MS/MS method.

Sample preparation. Each sample was prepared adding 10 µL of Working solution 1 to 100 µL of PBS or plasma. The obtained solutions correspond to 1 µM of analyte.

Each set of samples was incubated in triplicate at four different times, 0, 30, 60 and 120 min. at 37°C. Therefore, the degradation profile of analyte was represented by a batch of 12 samples (4 incubation times x 3 replicates). After the incubation, the samples were added with 300 µL of ISTD solution and

centrifuged. The supernatants were transferred in autosampler vials and dried under a gentle stream of nitrogen.

The dried samples were dissolved in 1.5 mL of mQ water/acetonitrile 80:20 added with 10 mM of formic acid. The obtained sample solutions were analysed by LC-MS/MS method described above.

Linearity and LOD. Calibration curve of analyte was obtained by plotting the peak area ratios (PAR), between quantitation ions of analyte and ISTD, versus the nominal concentration of the calibration solution. A linear regression analysis was applied to obtain the best fitting function between the calibration points.

The precision was evaluated through the relative standard deviation (RSD%) of the quantitative data of the replicate analysis of highest level of calibration curve.

In order to obtain reliable LOD values, the standard deviation of response and slope approach was employed.⁸⁴ The estimated standard deviations of responses were obtained by the standard deviation of y-intercepts (SDY-I) of regression lines. The obtained linear regressions, the linearity coefficients, precision and the estimated LOD values for the analyte are reported in Table 8.

Table 8. Linear regressions data, linearity coefficient, precision and LOD value.

Compd	Slope (PAR/ \square M)	Intercept (PAR)	R ²	Precision RSD	LOD (\square M)
10	0.805	0.045	0.992	3.5%	0.10

ASSOCIATED CONTENT

Supporting Information

- Combustion analysis data of the newly synthesized compounds and chemical degradation profiles of compound **10**, Ketoprofen Ethyl Ester (KEE) and Enalapril in different matrices. (PDF)

- PDB coordinates of the 3D structure of the hA_{2A}AR (PDB code 4EIY) that were added of hydrogen atoms and missing loop segments and energetically minimized. (PDB)
- PDB coordinates of the 3D structure of the hA₁AR (PDB code 5UEN) that were added of hydrogen atoms and missing loop segments and energetically minimized. (PDB)
- PDB coordinates of the homology model of the hA₃ adenosine receptor based on the hA₁ receptor X-ray structure (PDB code 5UEN) as a template. (PDB)
- Molecular formula strings. (CSV)

AUTHOR INFORMATION

Corresponding author

*Tel: +39 055 4573722. e-mail: daniela.catarzi@unifi.it.

ORCID

Daniela Catarzi [0000-0002-8821-928X](https://orcid.org/0000-0002-8821-928X)

Notes

The authors declare no competing financial interest.

ACKNOWLEDGMENTS. The work was financially supported by the Italian Ministry for University and Research (MIUR, PRIN 2010-2011, 20103W4779_004 project) and intramural Grant from the University of Florence (ex 60%).

ABBREVIATIONS USED

ABMECA, N⁶-(4-aminobenzyl)-N-methylcarboxamidoadenosine; Ado, Adenosine; AR, adenosine receptor; CCPA, 2-chloro-N⁶-cyclopentyladenosine; CHO, Chinese Hamster Ovary; CPA, N⁶-cyclopentyladenosine; DPCPX, 8-cyclopentyl-1,3-dipropylxanthine; EL, extracellular loop; HEPES, 4-(2-hydroxyethyl)-1-piperazineethanesulfonic acid; KEE, Ketoprofen Ethyl Ester; meca, mecamlamine; MLA, methyllycaconitine; MOE, molecular operating environment; nAChR, nicotinic acetylcholine receptor; NECA, 5'-(N-ethyl-carboxamido)adenosine; RMS, root-mean-square; TM, transmembrane.

References

1. Borea, P. A.; Gessi, S.; Merighi, S.; Varani, K. Adenosine as a multisignalling guardian angel in human diseases: when, where and how does it exert its protective effects? *Trends Pharmacol. Sci.* **2016**, *37*, 419–434.
2. Borea, P. A.; Gessi, S.; Merighi, S.; Vincenzi, F.; Varani, K. Pharmacology of adenosine receptors: the state of the art. *Physiol. Rev.* **2018**, *98*, 1591-1625.
3. Chen, J. F.; Eltzschig, H. K.; Fredholm, B. B. Adenosine receptors as drug targets – what are the challenges? *Nature Rev. Drug Discovery* **2013**, *12*, 265-286.
4. Stone, T. W.; Ceruti, S.; Abbracchio, M. P. Adenosine receptors and neurological disease: neuroprotection and neurodegeneration. *Handb. Exp. Pharmacol.* **2009**, *193*, 535-587.
5. Gomes, C. V.; Kaster, M. P.; Tomé, A. R.; Agostinho, P. M.; Cunha, R. A. Adenosine receptors and brain diseases: neuroprotection and neurodegeneration. *Biochim. Biophys. Acta* **2011**, *1808*, 1380-1399.
6. Müller, C. E.; Jacobson, K. A. Recent developments in adenosine receptor ligands and their potential as novel drugs. *Biochim. Biophys. Acta* **2011**, *1808*, 1290-1308.
7. Evans-Molina, C. Adenosine and seizures - What's the big fat deal? *Sci. Transl. Med.* **2011**, *3*, 92-113.
8. Rebola, N.; Simões, A. P.; Canas, P. M.; Tomé, A. R.; Andrade, G. M.; Barry, C. E.; Agostinho, P. M.; Lynch, M. A.; Cunha, R. A. Adenosine A_{2A} receptors control neuroinflammation and consequent hippocampal neuronal dysfunction. *J. Neurochem.* **2011**, *117*, 100-111.
9. Pinna, A.; Pontis, S.; Borsini, F.; Morelli, M. Adenosine A_{2A} receptor antagonists improve deficits in initiation of movement and sensory motor integration in the unilateral 6-hydroxydopamine rat model of Parkinson's disease. *Synapse* **2007**, *61*, 606–614.
10. Horiuchi, H.; Ogata, T.; Morino, T.; Yamamoto, H. Adenosine A₁ receptor agonists reduce hyperalgesia after spinal cord injury in rats. *Spinal Cord* **2010**, *48*, 685-690.
11. Sawynok, J. Adenosine receptor targets for pain. *Neuroscience* **2016**, *338*, 1-18.

- 1
2
3 12. Rivera-Oliver, M.; Díaz-Ríos, M. Using caffeine and other adenosine receptor antagonists and
4 agonists as therapeutic tools against neurodegenerative diseases: A review. *Life Sci.* **2014**, *101*, 1-9.
5
6
7 13. Bilkei-Gorzo, A.; Abo-Salem, O. M.; Hayallah, A. M.; Michel, K.; Müller, C. E.; Zimmer, A.
8 Adenosine receptor subtype-selective antagonists in inflammation and hyperalgesia. *Naunyn*
9 *Schmiedeberg's Arch. Pharmacol.* **2008**, *377*, 65-76.
10
11
12 14. Pechlivanova, D. M.; Georgiev, V. P. Effects of single and long-term theophylline treatment on
13 the threshold of mechanical nociception: contribution of adenosine A₁ and α 2-adrenoceptors.
14 *Methods Find. Exp. Clin. Pharmacol.* **2005**, *27*, 659-664
15
16
17 15. Gong, Q. J.; Li, Y. Y.; Xin, W. J.; Wei, X. H.; Cui, Y. Wang. J.; Liu, Y.; Liu, C. C.; Li, Y. Y.;
18 Liu, X. G. Differential effects of adenosine A₁ receptor on pain-related behavior in normal and nerve
19 injured rats. *Brain Res.* **2010**, *1361*, 23-30.
20
21
22 16. Katz, N. K.; Ryals, J. M.; Wright, D. E. Central or peripheral delivery of an adenosine A₁ receptor
23 agonist improves mechanical allodynia in mouse model of painful diabetic neuropathy. *Neuroscience*,
24 **2015**, *285*, 312-323.
25
26
27 17. Ferré, S; Diamond, I.; Goldberg, S. R.; Yao, L.; Hourani, S. M. O.; Huang, Z. L.; Urade, Y.;
28 Kitchen, I. Adenosine A_{2A} receptor in ventral striatum, hypothalamus and nociceptive circuitry.
29 Implication for drug addiction, sleep and pain. *Prog. Neurobiol.* **2007**, *83*, 332-347.
30
31
32 18. Cunha, R. A. Neuroprotection by adenosine in the brain: from A₁ receptor activation to A_{2A}
33 receptor blockade. *Purinergic Signal.* **2005**, *1*, 111-134.
34
35
36 19. Stockwell, J; Jakova, E.; Cayabyab, F. S. Adenosine A₁ and A_{2A} receptor in the brain: current
37 research and their role in neurodegeneration. *Molecules* **2017**, *22*, 676.
38
39
40 20. Dunwiddie, T. V.; Haas, H. L.; Adenosine increases synaptic facilitation in the in vitro rat
41 hippocampus: evidence for a presynaptic site of action. *J. Physiol.* **1985**, *369*, 365-377.
42
43
44 21. Alnouri, M. W.; Jepards, S.; Casari, A.; Schiedel, A. C.; Hinz, S.; Müller, C. E. Selectivity is
45 species-dependent: characterization of standard agonists and antagonists at human, rat, and mouse
46 adenosine receptors. *Purinergic Signal.* **2015**, *11*, 389-407.
47
48
49
50
51
52
53
54
55
56
57
58
59
60

- 1
2
3 22. Galeotti, N.; Ghelardini, C.; Grazioli, I.; Uslenghi, C. Indomethacin, caffeine and
4 prochlorperazine alone and combined revert hyperalgesia in vivo models of migraine. *Pharmacol.*
5
6 *Res.* **2002**, *46*, 245-250.
7
8
9
10 23. Wu, W. P.; Hao, J. X.; Fredholm, B. B.; Wiesenfeld-Hallin, Z.; Xu, X. J. Effect of acute and
11 chronic administration of caffeine on pain-like behaviors in rats with partial sciatic nerve injury.
12
13 *Neurosci. Lett.* **2006**, *402*, 164-166.
14
15
16
17 24. Sawynok, J. Caffeine and pain. *Pain* **2011**, *152*, 726-729.
18
19
20 25. Scott, J. R.; Hassett, A. L.; Brummett, C. M.; Harris, R. E.; Clauw, D. J.; Harte, S. E. Caffeine as
21 an opioid analgesic adjuvant in fibromyalgia. *J. Pain Res.* **2017**, *10*, 1801-1809.
22
23
24 26. Poli, D.; Catarzi, D.; Colotta, V.; Varano, F.; Filacchioni, G.; Daniele, S.; Trincavelli, L.; Martini,
25 C.; Paoletta, S.; Moro, S. The identification of the 2-phenylphthalazin-1(2H)-one scaffold as a new
26 decorable core skeleton for the design of potent and selective human A₃ adenosine receptor
27 antagonists. *J. Med. Chem.* **2011**, *54*, 2102–2113.
28
29
30
31
32
33 27. Squarcialupi, L.; Colotta, V.; Catarzi, D.; Varano, F.; Filacchioni, G.; Varani, K.; Corciulo, C.;
34 Vincenzi, F.; Borea, P. A.; Ghelardini, C.; Di Cesare Mannelli, L.; Ciancetta, A.; Moro, S. 2-
35 Arylpyrazolo[4,3- d]pyrimidin-7-amino derivatives as new potent and selective human A₃ adenosine
36 receptor antagonists. Molecular modeling studies and pharmacological evaluation. *J. Med. Chem.*
37
38 **2013**, *56*, 2256–2269.
39
40
41
42
43
44 28. Squarcialupi, L.; Colotta, V.; Catarzi, D.; Varano, F.; Betti, M.; Varani, K.; Vincenzi, F.; Borea,
45 P. A.; Porta, N.; Ciancetta, A.; Moro, S. 7- Amino-2-phenylpyrazolo[4,3-d]pyrimidine derivatives:
46 Structural investigations at the 5-position to target human A₁ and A_{2A} adenosine receptors. Molecular
47 modeling and pharmacological studies. *Eur. J. Med. Chem.* **2014**, *84*, 614–627.
48
49
50
51
52
53 29. Varano, F.; Catarzi, D.; Squarcialupi, L.; Betti, M.; Vincenzi, F.; Ravani, A.; Varani, K.; Dal Ben,
54 D.; Thomas, A.; Volpini, R.; Colotta, V. Exploring the 7-oxo-thiazolo[5,4-d]pyrimidine core for the
55 design of new human adenosine A₃ receptor antagonists. Synthesis, molecular modeling studies and
56 pharmacological evaluation. *Eur. J. Med. Chem.* **2015**, *96*, 105-121.
57
58
59
60

- 1
2
3 30. Catarzi, D.; Varano, F.; Poli, D.; Squarcialupi, L.; Betti, M.; Trincavelli, L.; Martini, C.; Dal Ben,
4 D.; Thomas, A.; Volpini, R.; Colotta, V. 1,2,4-Triazolo[1,5-a]quinoxaline derivatives and their
5 simplified analogues as adenosine A₃ receptor antagonists. Synthesis, structure–affinity relationships
6 and molecular modeling studies. *Bioorg. Med. Chem.* **2015**, *23*, 9–21.
7
8
9
10
11
12 31. Squarcialupi, L.; Catarzi, D.; Varano, F.; Betti, M.; Falsini, M.; Vincenzi, F.; Ravani, A.;
13 Ciancetta, A.; Varani, K.; Moro, S.; Colotta, V. Structural refinement of pyrazolo[4,3-d]pyrimidine
14 derivative to obtain highly potent and selective antagonists for the human A₃ adenosine receptor. *Eur.*
15 *J. Med. Chem.* **2016**, *108*, 117–133.
16
17
18
19
20
21 32. Varano, F.; Catarzi, D.; Vincenzi, F.; Betti, M.; Falsini, M.; Ravani, A.; Borea, P. A.; Colotta, V.;
22 Varani, K. Design, synthesis, and pharmacological characterization of 2-(2-furanyl)thiazolo[5,4-
23 d]pyrimidine-5,7-diamine derivatives: New highly potent A_{2A} adenosine receptor inverse agonists
24 with antinociceptive activity. *J. Med. Chem.* **2016**, *59*, 10564-10576.
25
26
27
28
29
30 33. Poli, D.; Falsini, M.; Varano, F.; Betti, M.; Varani, K.; Vincenzi, F.; Pugliese, A. M.; Pedata, F.;
31 Dal Ben, D.; Thomas, A.; Palchetti, I.; Bettazzi, F.; Catarzi, D.; Colotta, V. Imidazo[1,2-a]pyrazin-8-
32 amine core for the design of new adenosine receptor antagonists: Structural exploration to target the
33 A₃ and A_{2A} subtypes. *Eur. J. Med. Chem.* **2017**, *125*, 611-628.
34
35
36
37
38
39 34. Falsini, M.; Squarcialupi, L.; Catarzi, D.; Varano, F.; Betti, M.; Dal Ben, D.; Marucci, G.;
40 Buccioni, M.; Volpini, R.; De Vita, T.; Cavalli, A.; Colotta, V. The 1,2,4-Triazolo[4,3-a]pyrazin-3-
41 one as a versatile scaffold for the design of potent adenosine human receptor antagonists. Structural
42 investigations to target the A_{2A} receptor subtype. *J. Med. Chem.* **2017**, *60*, 5772-5790.
43
44
45
46
47
48 35. Varano, F.; Catarzi, D.; Vincenzi, F.; Falsini, M.; Pasquini, S.; Borea, P. A.; Colotta, V.; Varani,
49 K. Structure-activity relationship studies and pharmacological characterization of N5-
50 heteroarylalkyl-substituted-2-(2-furanyl) thiazolo[5,4-d]pyrimidine-5,7-diamine-based derivatives
51 as inverse agonists at human A_{2A} adenosine receptor. *Eur. J. Med. Chem.* **2018**, *155*, 552-561.
52
53
54
55
56
57
58
59
60

- 1
2
3 36. Catarzi, D.; Varano, F.; Falsini, M.; Varani, K.; Vincenzi, F.; Pasquini, S.; Dal Ben, D.; Colotta,
4
5 V. Development of novel pyridazinone-based adenosine receptor ligands. *Bioorg. Med. Chem.* **2018**,
6
7 28, 1484–1489.
- 8
9
10 37. Betti, M.; Catarzi, D.; Varano, F.; Falsini, M.; Varani, K.; Vincenzi, F.; Dal Ben, D.; Lambertucci,
11
12 C.; Colotta, V. The aminopyridine-3,5-dicarbonitrile core for the design of new non-nucleoside-like
13
14 agonists of the human adenosine A_{2B} receptor. *Eur. J. Med. Chem.* **2018**, *150*, 127-139
- 15
16
17 38. Beukers, M. W.; Chang, L. C. W.; von Frijtag Drabbe Kunzel, J. K.; Mulder-Krieger, T.;
18
19 Spanjersberg, R. F.; Brussee, J.; IJzerman, A. P. New, non-adenosine, high-potency agonists for the
20
21 human adenosine A_{2B} receptor with an improved selectivity profile compared to the reference agonist
22
23 N-ethylcarboxamidoadenosine. *J. Med. Chem.* **2004**, *47*, 3707–3079.
- 24
25
26 39. Chang, L. C. W.; von Frijtag Drabbe Künzel, J. K.; Mulder-Krieger, T.; Spanjersberg, R. F.;
27
28 Roerink, S. F.; van den Hout, G.; Beukers, M. W.; Brussee, J.; IJzerman, A. P. A series of ligand
29
30 displaying a remarkable agonistic-antagonistic profile at the adenosine A₁ receptor. *J. Med. Chem.*
31
32 **2005**, *48*, 2045-2053.
- 33
34
35 40. Meibom, D.; Albrecht-Küpper, B.; Diedrichs, N.; Hübsch, W.; Kast, R.; Krämer, T.; Krenz, U.;
36
37 Lerchen, H.-J.; Mittendorf, J.; nell, P. G.; Süßmeier, F.; Vakalopoulos, A.; Zimmermann, K.
38
39 neladenoson bialanate hydrochloride: a prodrug of a partial adenosine A₁ receptor agonist for the
40
41 chronic treatment of heart disease. *ChemMedChem* **2017**, *12*, 728-737.
- 42
43
44 41. Thimm, D.; Schiedel, A. C.; Sherbiny, F. F.; Hinz, S.; Hochheiser, K.; Bertarelli, D. C. G.; Maaß,
45
46 A.; Müller, C. E. Ligand-specific binding and activation of the human adenosine A_{2B} receptor.
47
48 *Biochemistry* **2013**, *52*, 726–740.
- 49
50
51 42. Dal Ben, D.; Buccioni, M.; Lambertucci, C.; Thomas, A.; Volpini, R. Simulation and comparative
52
53 analysis of binding modes of nucleoside and non-nucleoside agonists at the A_{2B} adenosine receptor.
54
55 *In Silico Pharmacol.* **2013**, *1*, 24.
- 56
57
58
59
60

- 1
2
3 43. Krivokolyko, S. G.; Dyachenko, V. D. Esters and nitriles of 3-phenylacrylic and 3-(2-furyl)acrylic
4 acid in synthesis of 6-amino-3,5-dicyano-4-phenyl(or 2-furyl)pyridine-2(1H)-thiones and –
5 selenones. *Ukrainskii Khimicheskii Zhurnal* **1996**, *62*, 61-66.
6
7
8
9
10 44. May, B. C. H.; Zorn, J. A.; Witkop, J.; Sherrill, J.; Wallace, A. C.; Legname, G.; Prusiner, S. B.;
11 Cohen, F. E.; Structure-activity relationship study of prion inhibition by 2-aminopyridine-3,5-
12 dicarbonitrile-based compounds: parallel synthesis, bioactivity, and in vitro pharmacokinetics. *J.*
13 *Med. Chem.* **2007**, *50*, 65-73.
14
15
16
17
18 45. Harada, H.; Watanuki, S.; Takuwa, T.; Kawaguchi, K.; Okazaki, T.; Hirano, Y.; Saitoh, C.
19 Preparation of Dicyanopyridine Derivatives as High-Conductance Calcium-Sensitive Potassium
20 Channel Openers. WO patent 06237 (A1), Jan 24, 2002.
21
22
23
24
25 46. Sridhar, M.; Ramanaiah, B. C.; Narsaiah, C.; Mahesh, B.; Kumaraswamy, M.; Mallu, K. K. R.;
26 Ankathi, V. M.; Shanthan Rao, P. Novel ZnCl₂-catalyzed one-pot multicomponent synthesis of 2-
27 amino-3,5-dicarbonitrile-6-thio-pyridines. *Tetrahedron Lett.* **2009**, *50*, 3897-3900.
28
29
30
31
32 47. Evdokimov, N. M.; Kireev, A. S.; Yakovenko, A. A.; Antipin, M. Y.; Magedov, I. V.; Kornienko,
33 A. One-step synthesis of heterocyclic privileged medicinal scaffolds by a multicomponent reaction
34 of malononitrile with aldehydes and thiols. *J. Org. Chem.* **2007**, *72*, 3443-3453.
35
36
37
38
39 48. Evdokimov, N. M.; Magedov, I. V.; Kireev, A. S.; Kornienko, A. One-step, three-component
40 synthesis of pyridines and 1,4-dihydropyridines with manifold medicinal utility. *Org. Lett.* **2006**, *8*,
41 899-902.
42
43
44
45
46 49. Eissa, A. M. F.; Ezz El-Arab, E. M.; Farag, A. M.; Moharram, H. H. Synthesis and biological
47 evaluation of pyrido[2,3.d]pyrimidine as antitumor effect. *Egyptian J. Chem.* **2006**, *49*, 761-774.
48
49
50
51 50. Brandt, W.; Mologni, L.; Preu, L.; Lemcke, T.; Gambacorti-Passerini, C.; Kunick, C. Inhibitors
52 of the RET tyrosine based on a 2-(alkylsulfanyl)-4-(3-thienyl)nicotinonitrile scaffold. *Eur. J. Med.*
53 *Chem.* **2010**, *45*, 2919-2927.
54
55
56
57
58
59
60

- 1
2
3 51. Attaby, F.; Elghandour A. H. H.; Ali, M. A.; Ibrahem, Y. M. Synthesis, reactions, and antiviral
4 activity of 6'-amino-2'-thioxo-1',2-dihydro-3,4'-bipyridine-3'-5'-dicarbonitrile. *Phosphorus, Sulfur*
5 *and Silicon and the Related Elements* **2007**, *182*, 695-709.
6
7
8
9
10 52. Cabrerizo, M. A.; Soto, J. L. Synthesis of heterocycles. III. 2-Amino-3,5-dicyano-4-aryl-6-
11 alkoxy pyridines from benzylidenemalononitriles. *Anales de Quimica* **1974**, *70*, 951-958.
12
13
14 53. Basyouni, W. M. Synthesis of novel substituted [1,2,4]triazolo[1,5-a]pyridines and their related
15 pyrano[2,3-d]imidazole derivatives. *Acta Chim. Slov.* **2003**, *50*, 223-238.
16
17
18
19 54. Dai, D.; Burgeson, J. R.; Tyavanagimatt, S. R.; Byrd, C. M.; Hrubby, D. E. Thienopyridine
20 Derivatives for the Treatment and Prevention of Dengue Virus Infections. US patent 0129677 (A1),
21 May 23, 2013.
22
23
24
25
26 55. Taliani, S.; Bellandi, M.; La Motta, C.; Da Settimo, F. A₃ receptor ligands: past, present and future
27 trends. *Curr. Topics Med. Chem.* **2010**, *10*, 942-975.
28
29
30
31 56. Glukhova, A.; Thal, D. M.; Nguyen, A. T.; Vecchio, E. A.; Jorg, M.; Scammells, P. J.; May, L.
32 T.; Sexton, P. M.; Christopoulos, A. Structure of the adenosine A₁ receptor reveals the basis for
33 subtype selectivity. *Cell* **2017**, *168*, 867-877.e13.
34
35
36
37 57. Molecular Operating Environment; C.C.G., I., 1255 University St., Suite 1600, Montreal, Quebec,
38 Canada, H3B 3X3.
39
40
41
42 58. Jones, G.; Willett, P.; Glen, R. C.; Leach, A. R.; Taylor, R. Development and validation of a
43 genetic algorithm for flexible docking. *J. Mol. Biol.* **1997**, *267*, 727-748.
44
45
46
47 59. Morris, G. M.; Goodsell, D. S.; Halliday, R. S.; Huey, R.; Hart, W. E.; Belew, R. K.; Olson, A. J.
48 Automated docking using a Lamarckian genetic algorithm and an empirical binding free energy
49 function. *J. Comput. Chem.* **1998**, *19*, 1639-1662.
50
51
52
53 60. Morris, G. M.; Huey, R.; Lindstrom, W.; Sanner, M. F.; Belew, R. K.; Goodsell, D. S.; Olson, A.
54 J. AutoDock4 and AutoDockTools4: Automated docking with selective receptor flexibility. *J.*
55 *Comput. Chem.* **2009**, *30*, 2785-2791.
56
57
58
59
60

- 1
2
3 61. Dallakyan, S.; Olson, A. J. Small-molecule library screening by docking with PyRx. *Methods*
4
5 *Mol. Biol.* **2015**, *1263*, 243-250.
6
7
8 62. Liu, W.; Chun, E.; Thompson, A. A.; Chubukov, P.; Xu, F.; Katritch, V.; Han, G. W.; Roth, C.
9
10 B.; Heitman, L. H.; IJzerman, A. P.; Cherezov, V.; Stevens, R. C. Structural basis for allosteric
11
12 regulation of GPCRs by sodium ions. *Science* **2012**, *337*, 232-236.
13
14
15 63. Dal Ben, D.; Buccioni, M.; Lambertucci, C.; Marucci, G.; Santinelli, C.; Spinaci, A.; Thomas, A.;
16
17 Volpini, R. Simulation and comparative analysis of different binding modes of non-nucleoside
18
19 agonists at the A_{2A} adenosine receptor. *Mol. Inform.* **2016**, *35*, 403-413.
20
21
22 64. Rodriguez, D.; Gao, Z. G.; Moss, S. M.; Jacobson, K. A.; Carlsson, J. Molecular docking
23
24 screening using agonist-bound GPCR structures: probing the A_{2A} adenosine receptor. *J. Chem. Inf.*
25
26 *Model* **2015**, *55*, 550-563.
27
28
29 65. Dal Ben, D.; Buccioni, M.; Lambertucci, C.; Marucci, G.; Thomas, A.; Volpini, R.; Cristalli, G.
30
31 Molecular modeling study on potent and selective adenosine A₃ receptor agonists. *Bioorg. Med.*
32
33 *Chem.* **2010**, *18*, 7923-7930
34
35
36 66. Congreve, M.; Andrews, S. P.; Dore, A. S.; Hollenstein, K.; Hurrell, E.; Langmead, C. J.; Mason,
37
38 J. S.; Ng, I. W.; Tehan, B.; Zhukov, A.; Weir, M.; Marshall, F. H. Discovery of 1,2,4-triazine
39
40 derivatives as adenosine A_{2A} antagonists using structure based drug design. *J. Med. Chem.* **2012**, *55*,
41
42 1898-1903.
43
44
45 67. Lebon, G.; Warne, T.; Edwards, P. C.; Bennett, K.; Langmead, C. J.; Leslie, A. G.; Tate, C. G.
46
47 Agonist-bound adenosine A_{2A} receptor structures reveal common features of GPCR activation.
48
49 *Nature* **2011**, *474*, 521-525.
50
51
52 68. Di Cesare Mannelli, L; Lucarini, E; Micheli, L; Mosca, I; Ambrosino, P; Soldovieri, M.V;
53
54 Martelli, A; Testai, L; Tagliatalata, M; Calderone, V; Ghelardini, C. Effects of natural and synthetic
55
56 isothiocyanate-based H₂S-releasers against chemotherapy-induced neuropathic pain: Role of Kv7
57
58 potassium channels. *Neuropharmacology* **2017**, *121*, 49-59.
59
60

- 1
2
3 69. Ribeiro, J. A.; Sebastião, A.M. Caffeine and adenosine. *J. Alzheimer Dis.* **2010**, *20* (Suppl 1), S3-
4
5 15.
6
7
8 70. Górska, A.M.; Gołembiowska, K. The role of adenosine A₁ and A_{2A} receptors in the caffeine
9
10 effect on MDMA-induced DA and 5-HT release in the mouse striatum. *Neurotox. Res.* **2015**, *27*, 229-
11
12 245.
13
14 71. Maltese, M.; Martella, G.; Imbriani, P.; Schuermans, J.; Billion, K.; Sciamanna, G.; Farook, F.;
15
16 Ponterio, G.; Tassone, A.; Santoro, M.; Bonsi, P.; Pisani, A.; Goodchild, R.E. Abnormal striatal
17
18 plasticity in a DYT11/SGCE myoclonus dystonia mouse model is reversed by adenosine A_{2A} receptor
19
20 inhibition. *Neurobiol. Dis.* **2017**, *108*, 128-139.
21
22
23 72. Bartolini, A.; Di Cesare Mannelli, L.; Ghelardini, C. Analgesic and antineuropathic drugs acting
24
25 through central cholinergic mechanisms. *Recent Pat. CNS Drug Discov.* **2011**, *6*, 119-140.
26
27
28 73. Ghelardini, C.; Galeotti, N.; Bartolini, A. Caffeine induces central cholinergic analgesia. *Naunyn*
29
30 *Schmiedebergs Arch. Pharmacol.* **1997**, *356*, 590-595.
31
32
33 74. Di Cesare Mannelli, L.; Ghelardini, C.; Calvani, M.; Nicolai, R.; Mosconi, L.; Toscano, A.;
34
35 Pacini, A.; Bartolini, A. Neuroprotective effects of acetyl-L-carnitine on neuropathic pain and
36
37 apoptosis: a role for the nicotinic receptor. *J Neurosci Res.* **2009**, *87*, 200-207.
38
39
40 75. Di Cesare Mannelli, L.; Pacini, A.; Matera, C.; Zanardelli, M.; Mello, T.; De Amici, M.;
41
42 Dallanoce, C.; Ghelardini, C. Involvement of $\alpha 7$ nAChR subtype in rat oxaliplatin-induced
43
44 neuropathy: effects of selective activation. *Neuropharmacology* **2014**, *79*, 37-48.
45
46
47 76. Vincenzi, F.; Targa, M.; Romagnoli, R.; Merighi, S.; Gessi, S.; Baraldi, P.G.; Borea, P.A.; Varani,
48
49 K. TRR469, a potent A₁ adenosine receptor allosteric modulator, exhibits anti-nociceptive properties
50
51 in acute and neuropathic pain models in mice. *Neuropharmacology* **2014**, *81*, 6-14.
52
53
54 77. Varani, K.; Massara, A.; Vincenzi, F.; Tosi, A.; Padovan, M.; Trotta, F.; Borea, P.A.
55
56 Normalization of A_{2A} and A₃ adenosine receptor up-regulation in rheumatoid arthritis patients by
57
58 treatment with anti-tumor necrosis factor alpha but not methotrexate. *Arthritis Rheum.* **2009**, *60*,
59
60 2880-2891.

- 1
2
3 78. Varani, K.; Merighi, S.; Gessi, S.; Klotz, K.-N.; Leung, E.; Baraldi, P.G.; Cacciari, B.; Romagnoli,
4 R.; Spalluto, G.; Borea, P.A. [³H]MRE 3008F20: a novel antagonist radioligand for the
5 pharmacological and biochemical characterization of human A₃ adenosine receptors, *Mol.*
6
7
8
9
10 *Pharmacol.* **2000**, *57*, 968-975.
- 11
12 79. Ravani, A.; Vincenzi, F.; Bortoluzzi, A.; Padovan, M.; Pasquini, S.; Gessi, .S.; Merighi, S.; Borea,
13 P.A.; Govoni, M.; Varani, K. Role and function of A_{2A} and A₃ adenosine receptors in patients with
14 ankylosing spondylitis, psoriatic arthritis and rheumatoid arthritis. *Int. J. Mol. Sci.* **2017**, *18*, 697.
- 15
16
17 80. McGrath, J.C. ; Lilley, E.. Implementing guidelines on reporting research using animals
18 (ARRIVE etc.): new requirements for publication in BJP. *Br. J. Pharmacol.* **2015**, *172*, 3189-3193.
- 19
20
21
22
23 81. Cavaletti, G.L.; Tredici, G.; Petruccioli, M.G.; Dondé, E.; Tredici, P.; Marmioli, P.; Minoia, C.;
24 Ronchi, A.; Bayssas, M.; Etienne, G.G. Effects of different schedules of oxaliplatin treatment on the
25 peripheral nervous system of the rat. *Eur. J. Cancer* **2001**, *37*, 2457-2463.
- 26
27
28
29
30 82. Di Cesare Mannelli, L.; Pacini, A.; Bonaccini, L.; Zanardelli, M.; Mello, T.; Ghelardini C.
31 Morphologic features and glial activation in rat oxaliplatin-dependent neuropathic pain. *J Pain.* **2013**,
32
33
34
35
36 *14*, 1585-1600.
- 37
38 83. Stewart, J. J. MOPAC: a semiempirical molecular orbital program. *J. Comput. Aided Mol. Des.*
39
40
41 **1990**, *4*, 1-105.
- 42
43 84. ICH Q2B, Validation of Analytical Procedure: Methodology, International Conference on
44 Harmonisation of Technical Requirements for Registration of Pharmaceuticals for Human Use, 1996.
45
46
47 <http://www.ich.org/products/guidelines/quality/article/quality-guidelines.html>, (accessed Nov 6,
48
49 1996).
- 50
51
52
53
54
55
56
57
58
59
60

Figure Captions.**Chart 1.**

Previously and currently reported amino-3,5-dicyanopyridines as AR ligands.

Figure 1. Competition curves of specific [³H]-DPCPX binding to hA₁ARs of compounds **9-12** (A). Increase of forskolin-stimulated cAMP levels in hA₁AR CHO cells by compounds **9-12** relative to the effect of DPCPX set at 100% (B). Data represent means ± SEM of four experiments each performed in triplicate.

Figure 2. A. Docking conformations of the synthesized compounds at the hA₁AR (PDB: 5UEN⁵⁶) cavity, taking **9** as template. Key receptor amino acids are indicated. **B.** Schematic view of the compound-receptor interaction (developed with the Ligand Interaction tool within MOE).

Figure 3. Top-view of the docking conformations of the synthesized compounds at the hA₁AR (PDB: 5UEN⁵⁶) binding site, taking **9** as example: detailed view of the interactions between the 6-substituent and the receptor aminoacids at the entrance of the binding cavity.

Figure 4. A-B. Ligand-target interaction energies calculated with the *IF-E 6.0* tool within MOE (see text for details) for sets of compounds differing only based on the 4-substituent. The receptor's amino acids located close to the 4-substituent were considered and are displayed in panel C. Data are represented as kcal mol⁻¹. The results show a significant interaction with Thr277^{7,42} for residues presenting a polar atom at the 3-endocyclic position within the 4-substituent (i.e. **19** and **26** in the first set and **18** and **24** in the second set). **C.** Detail of the ligand-target interaction at the 4-substituent (compound **26** is shown in this figure). The key residues (PDB: 5UEN⁵⁶) involved in this interaction are displayed and indicated.

1
2
3 **Figure 5.** A. Docking conformations of the synthesized compounds at the hA_{2A}AR cavity, taking
4 compound **9** (green) as template. Key receptor amino acids are indicated. The position of the 4-
5 heterocycle corresponds to the one of the 2-chlorophenol substituent of the 3-amino-1,2,4-triazine
6 derivative (red) co-crystallized with the hA_{2A}AR (pdb code: 3UZC⁶⁶). B. Top-view of the docking
7 conformations of the synthesized compounds at the A₁AR cavity, taking compound **9** as example:
8 detailed view of the interaction between the 6-substituent and the receptor aminoacids at the entrance
9 of the binding cavity. C. Binding mode of compound **17** at the hA₃AR cavity, analogue to the top-
10 score docking conformations at the hA₁AR and hA_{2A}AR. Key receptor residues are indicated. This
11 binding mode was observed only for some of the analyzed derivatives at the hA₃AR cavity.
12
13
14
15
16
17
18
19
20
21
22
23
24
25

26 **Figure 6.** Effects of selected compounds against neuropathic pain in mice. Neuropathy was induced
27 by repeated i.p. injection of oxaliplatin (2.4 mg kg⁻¹, daily). The hypersensitivity to a cold thermal
28 stimulus was measured on day 15 by the Cold plate test (latency to pain related behaviors as paw
29 lifting or licking). Compounds **9-12** were administered p.o, measurements were performed 15, 30,
30 45, and 60 min after. Control mice were treated with vehicle. Each value represents the mean of 10
31 mice per group, performed in 2 different experimental sets. **P < 0.01 vs vehicle + vehicle treated
32 mice. ^P < 0.05 and ^^P < 0.01 vs oxaliplatin + vehicle treated mice.
33
34
35
36
37
38
39
40
41
42
43

44 **Figure 7.** Effects of caffeine against neuropathic pain in mice. Role of nAChRs. Neuropathy was
45 induced by repeated i.p. injection of oxaliplatin (2.4 mg kg⁻¹, daily). The hypersensitivity to a cold
46 thermal stimulus was measured on day 15 by the Cold plate test (latency to pain related behaviors as
47 paw lifting or licking). Caffeine was administered p.o. at 10 mg kg⁻¹. The non-selective nAChR
48 antagonist mecamylamine (meca; 2 mg kg⁻¹ i.p.) and the selective alpha7 nAChR antagonist
49 methyllycaconitine (MLA; 6 mg kg⁻¹ i.p.) were administered 15 min before caffeine. Measurements
50 were performed overtime after the injection of caffeine or vehicle (in control mice). Values are
51 reported as mean of 10 mice per group (two different experimental sets). **P < 0.01 vs vehicle +
52
53
54
55
56
57
58
59
60

1
2
3 vehicle treated mice. $^{\wedge}P < 0.05$ and $^{\wedge\wedge}P < 0.01$ vs oxaliplatin + vehicle treated mice. $^{\circ}P < 0.01$ vs
4
5 oxaliplatin + caffeine treated mice.
6
7
8

9 **Figure 8.** Effects of nicotinic antagonisms on compound **9** anti-hyperalgesic efficacy. Neuropathy
10 was induced by repeated i.p. injection of oxaliplatin (2.4 mg kg⁻¹, daily). The hypersensitivity to a
11 cold thermal stimulus was measured on day 15 by the Cold plate test (latency to pain related behaviors
12 as paw lifting or licking). The non-selective nAChR antagonist mecamylamine (meca; 2 mg kg⁻¹ i.p.)
13 and the selective alpha7 nAChR antagonist methyllycaconitine (MLA; 6 mg kg⁻¹ i.p.) were
14 administered 15 min before **9** (0.3 mg kg⁻¹ p.o.). Measurements were performed overtime after the
15 injection of **9** or vehicle (in control mice). Values are reported as mean of 10 mice per group (two
16 different experimental sets). $^{**}P < 0.01$ vs vehicle + vehicle treated mice. $^{\wedge}P < 0.05$ and $^{\wedge\wedge}P < 0.01$
17 vs oxaliplatin + vehicle treated mice. $^{\circ}P < 0.01$ vs oxaliplatin + **9** treated mice.
18
19
20
21
22
23
24
25
26
27
28
29
30
31

32 **Figure 9.** Effects of nicotinic antagonisms on **10** anti-hyperalgesic efficacy. Neuropathy was induced
33 by repeated i.p. injection of oxaliplatin (2.4 mg kg⁻¹, daily). The hypersensitivity to a cold thermal
34 stimulus was measured on day 15 by the Cold plate test (latency to pain related behaviors as paw
35 lifting or licking). The non-selective nAChR antagonist mecamylamine (meca; 2 mg kg⁻¹ i.p.) and the
36 selective alpha7 nAChR antagonist methyllycaconitine (MLA; 6 mg kg⁻¹ i.p.) were administered 15
37 min before **10** (0.3 mg kg⁻¹ p.o.). Measurements were performed overtime after the injection of **10** or
38 vehicle (in control mice). Values are reported as mean of 10 mice per group (two different
39 experimental sets). $^{**}P < 0.01$ vs vehicle + vehicle treated mice. $^{\wedge}P < 0.05$ and $^{\wedge\wedge}P < 0.01$ vs
40 oxaliplatin + vehicle treated mice. $^{\circ}P < 0.01$ vs oxaliplatin + **10** treated mice.
41
42
43
44
45
46
47
48
49
50
51
52
53
54
55
56
57
58
59
60

1
2
3 **Scheme 1.**
4

5 **Reagents and conditions.** a) Malononitrile, thiophenol, TBAF, H₂O, 80 °C; b) Na₂S, anhydrous
6 DMF, 80 °C; 1N HCl, rt; c) R³CH₂Br, NaHCO₃, anhydrous DMF, rt; d) NH₂COCH₂Cl, 10% KOH,
7 DMF, rt (compound **5**); e) NH₂CH₂CH₂OH, DMF, 100 °C; (for R³ substituent details see Table 1).
8
9
10
11
12
13

14 **Scheme 2.**
15

16 **Reagents and conditions.** a) malononitrile, NaOCH₃, TBAF, MeOH, reflux; b) 12N HCl, glacial
17 AcOH, 100 °C; c) BrCH₂CH₂OH, NaHCO₃, anhydrous DMF, 80 °C, microwave irradiation.
18
19
20
21
22

23 **Scheme 3.**
24

25 **Reagents and conditions.** a) isoamylnitrite, CuCl₂, CH₃CN, rt; b) R¹-NH₂, anhydrous DMF, rt.
26
27
28

29 **Scheme 4.**
30

31 **Reagents and conditions.** a) acetic anhydride, pyridine, reflux; b) Na₂S, anhydrous DMF, 50 °C; 1N
32 HCl, rt; c) BrCH₂CH₂OH, NaHCO₃, anhydrous DMF, rt.
33
34
35
36
37
38
39
40
41
42
43
44
45
46
47
48
49
50
51
52
53
54
55
56
57
58
59
60

1
2
3 **Table of Contents Graphic**
4
5
6

